IDENTIFICATION OF THE GENE RESPONSIBLE FOR PULMONARY ALVEOLAR MICROLITHIASIS AND POSSIBLY ASSOCIATED WITH TESTICULAR MICROLITHIASIS

by

Ayşe Corut

B.S., Molecular Biology and Genetics, Boğaziçi University, 2003

Submitted to the Institute for Graduate Studies in
Science and Engineering in partial fulfillment of
the requirements for the degree of
Master of Science

Graduate Program in Molecular Biology and Genetics
Boğaziçi University

2006

ACKNOWLEDGMENTS

I have a great pleasure in thanking my thesis supervisor Prof. Aslı Tolun for sharing her endless knowledge with me, her constructive criticisms, encouragement and guidance throughout the study.

I would like to express my gratitude to the members of my thesis committee Prof. Nejat Dalay and Prof. Nazlı Başak for sparing their valuable time to evaluate this work.

This work would not have been possible without the help and support of Sibel Uğur, from whom I have learned all aspects of laboratory work. I also feel very lucky in establishing a strong friendship with my group friends, Nadire Duru and Murat Çetinkaya with whom I have worked in harmony and shared valuable experience for almost three years. I also want to thank project students İbrahim Ilık and Minal Çalışkan for their help in the laboratory.

I have particularly great pleasure in thanking all members of MBG and in particular Mine Güzel and Sinem Hocaoğlu for being such great friends.

I also thank to the patient families for participating in this study. The grant from the State Planning Organization is greatly acknowledged.

Last, but certainly not least, I would like to thank my family for their guidance, understanding, patience and continuous moral support throughout my entire education.

I am also very grateful for having other excellent friends such as Erdem, Gamze, Pelin and Merve who are full of love, support and endless patience for me despite the very long working hours that kept me away from their company.

ABSTRACT

IDENTIFICATION OF THE GENE RESPONSIBLE FOR PULMONARY ALVEOLAR MICROLITHIASIS AND POSSIBLY ASSOCIATED WITH TESTICULAR MICROLITHIASIS

In this study two inherited disorders, namely pulmonary alveolar microlithiasis (PAM) and testicular microlithiasis (TM), were studied. PAM is a rare autosomal disease characterized by the deposition of calcium phosphate microliths throughout the lungs. TM is a more common disorder that is thought to follow a complex pattern of inheritance often associated with infertility and cancer.

Autozygosity (homozygosity) mapping was used to fine-map the disease gene responsible for PAM resulting from parental consanguinity in a large Anatolian family. Computer based parametric tests were applied to evaluate the linkage information obtained by autozygosity mapping and confirmed gene localization. Later, positional candidate gene approach assessed *SLC34A2* or *type IIb sodium-phosphate cotransporter* as the gene responsible for PAM.

In this study, SSCP assay was employed to screen *SLC34A2* for disease causing mutations in PAM patients. A total of five homozygous exonic mutations were identified in six unrelated PAM patients showing that impaired activity of the phosphate transporter *SLC34A2* is presumably responsible for the alveolar microliths. Since the gene is also expressed in testis, using SSCP and subsequent DNA sequencing analysis, mutations were searched in 15 TM subjects and two rare variants identified.

ÖZET

PULMONER ALVEOLAR MİKROLİTİYAZİSTEN SORUMLU VE TESTİKÜLER MİKROLİTİYAZİSLE MUHTEMELEN İLİŞKİLİ BİR GENİN BULUNMASI

Bu çalışmada pulmoner alveolar mikrolitiyazis (PAM) ve testiküler mikrolitiyazis (TM) isimli iki kalıtsal hastalık çalışılmıştır. PAM akciğerde kalsiyum fosfat mikrotaşlarının birikme özelliği gösterdiği nadir rastlanan bir hastalık iken, TM daha karmaşık bir şekilde kalıtılan, genellikle kısırlık ve kanserle seyreden ve sık rastlanan bir hastalıktır.

Büyük bir Anadolu ailesindeki akraba evliliklerine bağlı olarak gözlemlediğimiz otozomal resesif PAM hastalığının yerini daraltmak için homozigot haritalaması kullanılmıştır. Bilgisayar destekli parametrik testler çekinik bir hastalık olan PAM'ın homozigotluk haritalaması yöntemiyle elde edilen bağlantı bilgilerinin değerlendirilmesi amacıyla uygulanmıştır. Daha sonra, konuma bağlı aday gen yaklaşımıyla *SLC34A2,* ya da *tip IIb sodyum-fosfat kotransportör*, PAM'dan sorumlu tek aday gen olarak değerlendirilmiştir.

PAM hastalığına yol açan *SLC34A2* mutasyonlarını aramak için SSCP uygulanmıştır. Aralarında akrabalık ilişkisi bulunmayan altı PAM hastasında, bozuk *SLC34A2* aktivitesinin alveollerdeki mikrotaşlardan sorumlu olduğunu gösteren toplam beş farklı homozigot ekzonik mutasyon saptanmıştır. Aynı gen testislerde de eksprese edildiğinden, SSCP ve DNA dizileme yöntemiyle onbeş TM hastasında bu gende mutasyon aranmıştır. İki nadir varyant saptanmıştır.

TABLE OF CONTENTS

LIST OF FIGURES

LIST OF TABLES

LIST OF ABBREVIATIONS

A	Adenine
bp	Base pair
C	Cytosine
cAMP	Cyclic adenosine monophosphate
CDS	Coding sequence
CEPH	Centre d'Étude du Polymorphisme Humain
cGMP	Cyclic guanosine monophosphate
cM	Centimorgan
ddNTP	Dideoxynucleoside triphosphate
DNA	Deoxyribonucleic acid
EDTA	Ethylenediaminetetraacetate
G	Guanine
IBD	Identical by descent
kb	Kilobase
kDa	Kilodalton
Lod	Log of odds
Mb	Megabase
MDE	Mutation detection enhancement
min	Minute
MLE	Maximum likelihood estimate
MLS	Maximum lod score
mRNA	Messenger ribonucleic acid
PAM	Pulmonary alveolar microlithiasis
PCR	Polymerase chain reaction
R	Arginine
rpm	Revolution per minute
SLC34A2	Type IIb sodium-phosphate cotransporter
SNP	Single nucleotide polymorphism
SSCP	Single strand conformation polymorphism
T	Thymine

TEMED	N, N, N, N'-Tetramethylethylenediamine
TM	Testicular microlithiasis
U	Unit
UTR	Untranslated region
UV	Ultraviolet

1. INTRODUCTION

In this study, genetic analyses were performed in order to refine the locus for the autosomal recessive disorder pulmonary alveolar microlithiasis (PAM) and to identify the genes responsible for that disease and the disorder testicular microlithiasis (TM) with unknown pattern of inheritance.

Initial genetic studies had been performed in our laboratory for PAM families that roughly mapped the PAM locus to chromosome 4p. In this study, PAM locus was refined to a 4.2 Mega base (Mb) interval flanked by markers D4S1533 and D4S2305. SLC34A2 gene was assessed as the strongest candidate among the 24 genes localized within the gene locus. Further investigation of the gene revealed mutations in the PAM patients and variations in the TM patients analyzed.

1.1. Pulmonary Alveolar Microlithiasis

Pulmonary alveolar microlithiasis is a rare disorder of unknown etiology. It is characterized by the formation and accumulation of innumerable, intra-alveolar, roundish tiny corpuscles called 'microliths' (Prakash et al., 1983). This eventually leads to deterioration of the lungs. There is no cure or treatment except for lung transplantation (Stamatis et al., 1993).

Italian scientist Marcello Malpighi was the first to give a precise macroscopic description of the disease in 1686 (Malpighi et al., 1966). Three centuries later, chemical analysis together with energy dispersion X-ray microanalysis showed that the microliths, being composed of calcium and phosphate (in a ratio of 2 to 1) varied in size from 0.01 up to 3 mm in diameter (Rabin et al., 1980; Wineselberg et al., 1984; Pracyk et al., 1996). Interestingly, the name of the disease was given by the Hungarian pathologist Lajos Puhr in 1933 (Puhr et al., 1933), much later than Marcello Malpighi who had described PAM as 'In vesciculis pulmonum innumeri lapilli sunt', meaning 'Innumerable number of little stones in the lung'.

PAM is believed to follow a homozygous recessive pattern of inheritance (Burguet et al., 1967; Passariello et al., 1968; Enacar et al., 1977; Şenyiğit et al., 2001). However, some physicians believe that the disease results mainly due to environmental factors (Felson et al., 1988; Nouh et al., 1989; Biary et al., 1993).

There is no particular continental restriction for the disease, but the highest number of cases was reported in Europe (157 of 424 cases: 37.02%) and Asia (153 cases: 36.08%), respectively. A reporting bias due to a better quality of clinicians in Europe cannot be ruled out. The nation with the highest number of reported cases of PAM is Turkey with 69 cases (16.27%) (Uçan et al., 1993; Şenyiğit, 2001), followed by Italy with 56 cases (13.2%) (Perosa and Ramunni, 1959; Mariotta et al., 1997) and USA with 38 cases (8.96%). Among the total cases, 269 were sporadic (63.44%) showing a higher prevalence of the male sex (138 males: 61.3%, 87 females: 38.7%, 44 unspecified), while 155 were familial showing similar proportions in both sexes (70 males: 46.35%, 81 females: 53.65%, 4 unspecified). In sporadic cases the bias in male sex is attributed to more frequent X-ray examinations of the male patients for civil reasons such as military service or health reasons such as a higher involvement with the respiratory diseases (Castellana et al., 2002; Castellana et al 2003).

Chi-square analysis performed in this study showed that the larger number of males than females in the sporadic cases were significant ($p<0.01$) in contrast to the familial cases ($0.2<p<0.5$). The discrepancy most likely results, as explained above, from a higher X-ray examination rate for males. Family screening after the diagnosis of a single member generally detects familial cases.

In the familial cases, sibling affection seems to dominate, rendering the homozygous recessive inheritance model very likely (Burguet et al., 1967; Passariello et al., 1968; Enacar et al., 1977; Şenyiğit et al., 2001).

The majority of PAM patients are asymptomatic at the time of diagnosis. Lack of clinical symptoms was observed as late as 41 years after diagnosis (Prakash et al., 1983). The progression of the disease is generally very slow, but as it progresses, the first symptom to develop is dyspnea (difficulty in breathing) on exertion, which is frequently

absent even when almost the entire lung parenchyma is involved. Therefore, it is not the clinical symptoms but the so-called sand storm appearance of the numerous tiny nodular opacities in lower lung zones visualized with chest radiography (Figure 1.1) (Cluzel et al., 1991). Lack of clinical symptoms also leads to late onset of the disorder, and the diagnosis is usually made incidentally in patients undergoing X-ray analysis for other reasons.

Figure 1.1. Sandstorm-lung appearance observed in the chest radiograph of a PAM patient. Fine microliths with a diffuse and uniform spreading pattern are observed in the cardiac and diaphragmatic borders (Taken from Castellana et al., 2002).

Since the genetic basis of the disease was unknown, several proposals were made to explain the etiology. According to the proposed mechanism for intra-alveolar microlith formation, stimuli or secretions of unknown origin increased the alkalinity of the alveolar lining, promoting the intra-alveolar precipitation of calcium phosphates and carbonates (Bogart et al., 1980).

1.2. Testicular Microlithiasis

Testicular microlithiasis is a rare, generally asymptomatic, slowly progressing disorder of the seminiferous tubules of testis (Priebe et al., 1970). The pattern of inheritance of the disease has not been studied. The disease is characterized by the intra-tubular microliths consisting of calcified central cores that are surrounded by concentric

layers of cellular debris, glycoprotein and collagen (Vegni-Talluri et al., 1980). They are often an incidental finding in ultrasound examination of the scrotum and seen as multiple non-shadowing, scattered echogenic foci that are 1-3 mm in diameter (Figure 1.2) (Doherty et al., 1987). The chemical composition of the microliths is hydroxyapatite, a form of calcium phosphate (De Jong et al., 2004). There are various hypotheses on the mechanism of microlith formation, but none has been widely accepted (Bieger et al., 1965; Vegni-Talluri et al., 1980; Bushby et al., 2002).

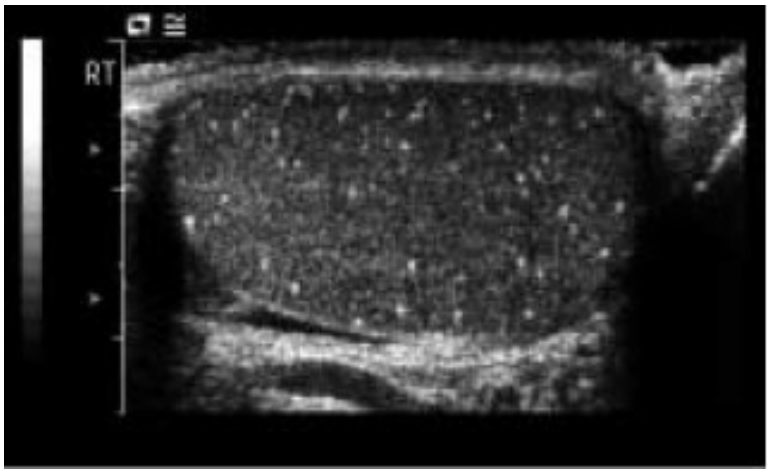

Figure 1.2. Typical ultrasound appearance of testicular microlithiasis with high reflective areas of microlithiasis on the background of a low reflective testis. (Taken from Doherty et al., 1987).

This rare disease of unknown etiology was found also in association with cryptorchidism (Nistal et al., 1979), delayed testicular descent (Mullins et al., 1986), testicular torsion (Jaramillo et al., 1989), PAM (Coetzee et al., 1970; Arslan et al., 1996), varicocoele (Janzen et al., 1992), multiple lentigines (Leman et al., 2000), neurofibromatosis (Ganem et al., 1999), Klinefelter syndrome (Aizenstein et al., 1997), male pseudohermaphroditism (Khan et al., 2000) and male sub-fertility (Ganem et al., 1999). However, special concern is due to its possible association with testicular germ cell cancer (Bennett et al., 2001) and intratubular germ cell neoplasia (Parra et al., 1996).

1.3. The SLC34A2 (Type IIb Na-Pi cotransporter) Gene

Inorganic phosphate (P_i) is known to play a role in cellular metabolism, bone formation, development and growth. The control of inorganic phosphate metabolism and phosphate homeostatis depends mainly on the absorption of P_i from the small intestine but also from renal tubules. In lung, *type IIb Na-Pi cotransporter* is expressed in ATII cells, and this cotransporter is located at the apical cell membrane. The abundance of the type IIb cotransporter in such a location suggests an involvement in the reuptake of phosphate necessary for the synthesis of surfactant (Traebert et al., 1999).

A number of structurally distinct and functionally related sodium-dependent phosphate transporters have been identified. They are subtyped into 3 groups based on sequence homology. Type 1 transporters that do not seem to be regulated by dietary phosphate levels are found mainly in kidney. Type 2 transporters are divided into two, with first subgroup being expressed almost exclusively in the renal proximal tubule and the second in various other tissues. The cellular function of type 3 transporters is not known.

Human *SLC34A2*, a member of the solute carrier family 34A, is a type 2b P_i-transporter encoding gene, known to map to 4p15.1-p15.3. The 2.11 kb gene transcript is highly expressed in adult and fetal lung and less so in several other tissues of epithelial origin such as testis, small intestine, pancreas, kidney and prostate. The gene is predicted to encode a protein of 690 amino acids with 8 transmembrane domains and having a strong functional activity in direct correlation with increasing pH. The gene consists of 13 exons that vary between 40 - 615 nucleotides in length, whereas the introns are within a range of 92 - 6608 nucleotides. The first exon of the gene is non-coding.

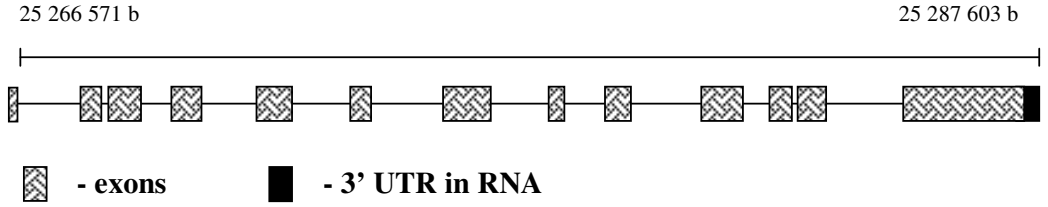

Figure 1.3. The structure of *SLC34A2*

1.4. Genetic Linkage and Lod Score Analysis

Distance between genetic loci can be estimated by linkage analysis, a statistical technique that relies on the fact that two loci that lie close to each other on the same chromosome tend to be inherited together. The closer the loci are, the greater the likelihood that they will be passed on to offspring as a pair. Even closely linked loci, however, can be separated by recombination during meiosis. The larger the distance between two genetic loci, the greater is the chance that they will be separated by a crossover. The frequency with which recombination occurs, namely, the recombination fraction that is denoted θ, increases with the distance between loci. If the loci are far apart, the probabilities of recombinant and parental chromosomes are equal, that is $\theta = 0.5$, just as when loci are on different chromosomes. Therefore, it is logical to use recombination events between genetic markers that are closely spaced on a chromosome to find a gene responsible for a disease within a relatively narrow length of DNA. However, recombination frequency does not reveal the exact physical distance between two loci but is only a measure of genetic distance. Two loci that show 1 per cent recombination frequency are defined to be 1 centimorgan (cM) apart on the genetic map. One cM corresponds very roughly to one megabase of DNA.

Based on the observed association between two loci in a given family, a statistical test of linkage analysis is utilized. The test is Lod (**l**og of **od**ds) Score Analysis introduced by Morton (1955) and discriminates between two hypotheses: the null hypothesis of no linkage ($\theta = 0.5$) and the alternative hypothesis of linkage ($\theta < 0.5$). The statistical criterion for concluding linkage between two traits is based on an observed odds ratio "L", which is the ratio of the probability of observing the distributional pattern of the two traits in a given family with linkage at θ to the same probability under the hypothesis of no linkage at $\theta = 0.5$ (Risch, 1992). The decimal logarithm of L, namely, the lod score denoted by the function $Z(\theta)$, is calculated at several values of θ, and the maximum test statistics of Z-maximum likelihood lod score (MLS) is reported. The θ value, which gives the MLS, is the maximum likelihood estimate (MLE) of θ.

For two genetic markers, the threshold for accepting that there is genetic linkage is set at a lod score of 3.0, corresponding to an odds ratio of 1000 to 1. The threshold for

rejecting linkage is set at a lod score of –2.0, whereas lod score values between –2.0 and 3.0 are inconclusive (Nyholt, 2000).

Lod score analysis requires a genetic model with clearly defined parameters, such as the mode of inheritance, the degree of penetrance, and the frequencies of alleles. Since lod scores are logarithmic, the data from more than one family can be combined in this test by directly adding Lod scores from different families for a particular trait.

1.5. Autozygosity Mapping

Autozygosity is a form of genetic mapping for autosomal recessive disorders in which affected individuals are expected to have two disease alleles identical by descent i.e., inherited from a common ancestor. Autozygosity mapping is based on the idea that affected individuals for an autosomal recessive trait whose parents are related most likely have received a common haplotype without recombination and in the homozygous state from a single ancestor (Lander and Botstein, 1987).

A person afflicted with a rare recessive disease and with consanguineous parents is likely to be autozygous for markers linked to the disease locus, because the frequency of the trait is so low that the disease can only arise due to consanguinity. In such cases, it is very likely that the affected individuals in the population are homozygous by descent. Therefore, inbred families are of great value for linkage studies, since even a single family can yield a significantly high lod score. Moreover, autozygosity mapping can be a solution in mapping diseases with locus heterogeneity whenever large inbred families are present.

In summary, autozygosity mapping can be a very powerful tool in especially some regions of the world where inbreeding is very common. In the Anatolian population, for example, it has been estimated that 21 per cent of the marriages are consanguineous, with first-cousin marriages as the most common type (Başaran *et al.*, 1998).

1.6. DNA Analyses

1.6.1. Polymerase Chain Reaction

Polymerase chain reaction (PCR) is an in-vitro methodology that is based on the use of enzyme DNA polymerase to copy a DNA template in repeated rounds of replication. The polymerase is guided to the sequence to be copied by short primer oligonucleotides that are hybridized to the DNA template at the beginning and the end of the target DNA sequence. In other words, these designed primers determine the segment of DNA to be amplified.

In a PCR reaction, each repeated round of replication is defined as a cycle. A cycle consists of 3 steps, with the first step heat-denaturing the double stranded DNA into the single stranded form. The second step is the annealing of primers to the DNA template, followed by DNA synthesis starting from each of the primers. In this study all DNA methods employed were based on PCR.

1.6.2. Genotyping with Microsattelite Markers

Linkage analysis involves the usage of genetic markers that are short DNA sequences dispersed throughout the whole genome. Various kinds of genetic markers such as restriction enzyme fragment length polymorphisms (RFLPs), single nucleotide polymorphisms (SNPs), minisatellites and macrosatellites can be used to construct a genetic map in a linkage study. RFLPs have two alleles at the most. SNPs are similar to RFLPs, but they very commonly consist of nucleotide variances that do not create or abolish restriction sites.

One of the problems in linkage studies is the limited informativeness of the markers used. The members of the family under study should ideally carry two different alleles each. Therefore, highly polymorphic markers are most suitable for gene mapping. A polymorphic marker displays two or more alleles, and by definition the more common allele of a biallelic marker should have a frequency at the most 0.99. Hence, in a linkage study, both RFLP and SNP markers that are biallelic can be uninformative most of the

time. Therefore, microsatellite markers (Weissenbach *et al.*, 1992) that are abundant, highly polymorphic and easy to assay are preferrable in linkage studies. On the contrary, hypervariable minisatellite markers, despite their high polymorphism, do not serve as tools for genome-wide linkage analysis, as they tend to cluster mostly near telomeric regions and their large alleles cannot be amplified easily by PCR.

In this study, microsattelite markers were used for haplotype analysis in order to construct a haplotype pedigree of the PAM family and thereby to refine the gene locus on chromosome 4p.

1.6.3. Single Stranded Conformational Polymorphism (SSCP) Technique

SSCP is a non-denaturing gel electrophoresis technique in which a highly cross-linked gel of polyacrylamide is used as an inert matrix through which DNA molecules migrate. The gel is non-denaturing, since it is run at a low temperature without denaturing agents. Pre-denatured single stranded DNA molecules of interest gain their secondary conformation in the gel during electrophoresis. Therefore, single stranded DNA fragments that differ in sequence length or in nucleotide composition display shifts in mobility on the gel, yielding 4 bands in the heterozygotes and 2 in the homozygotes.

In this study, among all genes at the gene locus, *SLC34A2* was assessed as the strongest candidate to be responsible for PAM and TM. To investigate any variations and mutations in *SLC34A2*, SSCP technique was applied to affected and healthy individuals.

SSCP technique has an efficiency of about 70 per cent. Therefore, an absence of a band shift does not exclude a sequence difference in a DNA sample. However, any difference in the SSCP pattern indicates a sequence difference that needs to be further investigated by DNA sequence analysis. Hence, in this study, DNA sequencing was applied to fragments exhibiting different band patterns on the SSCP gel.

1.6.4. DNA Sequence Analysis

DNA sequencing relies on the use of dideoxyribonucleoside triphosphates (ddNTPs) that lack the 3' hydroxyl group. The method allows the nucleotide sequence of a purified DNA fragment to be determined simply and quickly. DNA is synthesized by PCR in a mixture that contains only a single oligonucleotide primer, the enzyme DNA polymerase, a mixture of deoxyribonucleoside triphosphates (dNTP) and a particular ddNTP. Once a ddNTP is incorporated into a growing DNA chain, due to the lack of 3'OH, the addition of the next nucleotide is blocked, resulting in the termination of DNA synthesis. This reaction produces a set of DNAs of various lengths complementary to the template DNA that is being sequenced. To determine the complete sequence of a DNA fragment, four different reaction mixtures are prepared, each containing a different ddNTP. The products of each of these reaction mixtures are loaded to four parallel lanes of a polyacrylamide gel and resolved by electrophoresis. The bands in each lane represent fragments that have been terminated at a dideoxynucleotide at various positions. Starting from the bottom of the gel, working across all lanes, the DNA sequence of the newly synthesized strand that is complementary to the template DNA can be determined.

This basic method is still applied today but with several improvements, so that DNA sequencing is now completely automated. Robotic devices mix the reagents, then load, run and read the order of the fragments. Different colored fluorescent dyes are used to label each type of ddNTP so that reactions for all four ddNTPs can be run together in a single lane. A detector reads the gel and records the four labels. A computer then interprets and stores the sequence information.

1.7. Patterns of Inheritance

The studies of Gregor Mendel, the father of modern genetics, showed that inheritance is based on the transmission of a trait in either a dominant or a recessive fashion. Later, together with X-linked pattern, this type of inheritance is defined as Mendelian pattern of inheritance. However, it is not always solely a single gene that is responsible for a phenotype. A trait can be biallelic or multiallelic meaning that there are

several possible alleles at the same locus. Each individual has only 2 autosomal alleles, and only one is transmitted to a gamete.

Discoveries on DNA structure, the genetic code and the genome and the observation that some traits including hereditary disorders do not follow classical Mendelian inheritance have led researchers to define other patterns of transmission for autosomal traits. They are called non-Mendelian or complex inheritance. Complex inheritance is based on the synergy of more than one gene and/or environmental factors. Impaired activity of more than one gene could predispose for a disease, and the effects of the environment could additionally contribute. Hence, inheritance of complex traits is more difficult to study in comparison to monogenic traits.

Another kind of non-Mendelian inheritance is not autosomal but mitochondrial, a pattern of genetic transmission that is strictly maternal. Especially in higher animals, egg cell always contributes much more cytoplasm to the zygote as compared to sperm. Therefore, it is expected that inheritance of mitochondria by the zygote is nearly uniparental, or more specifically maternal. Hence, a mitochondrial disease is transmitted solely from a female to her descendants. An inherited disease of mitochondrial origin is best understood by its transmission from affected females to daughters and sons, with the daughters but not the sons giving rise to affected offspring.

In this study, we showed that PAM is an autosomal recessive disease that follows Mendelian laws of genetics by showing that all PAM patients carry homozygous mutations for *SLC34A2*. We further propose that TM is a non-Mendelian disorder, since variations in *SLC34A2* were observed in only one allele of some of the TM patients, indicating that the gene can only partially contribute to this disease.

2. PURPOSE

In the first part of this study, the purpose was to refine the linkage profile of the autosomal recessive disorder PAM at chromosome location 4p by taking advantage of the homozygousity mapping and computer programs developed for parametric linkage tests. Subsequently, assuming to follow a complex pattern of inheritance, another disorder TM was analyzed for the disease region defined for PAM. In the first part of the study, the aims were:

- Refine the disease locus for PAM,
- Investigate linkage of *SLC34A2* to disorder PAM by using computer programs,
- Investigate whether the gene locus is partially responsible for TM.

In the second part of the study, the aims were to conduct candidate gene approach in order to detect:

- Causative mutations responsible for PAM
- Variants possibly associated with TM in *SLC34A2,* encoding typeIIb sodium dependent phosphate transporter.

3. MATERIALS

3.1. Subjects

Peripheral blood samples from seven PAM patients and families afflicted with Pulmonary Alveolar Microlithiasis were provided by clinicians Abdurrahman Şenyiğit, Sedat Altın, Uğur Özçelik, Haluk Çalışır, Zeki Yıldırım and Ayhan Göçmen.

Peripheral blood samples from fifteen Testicular Microlithiasis patients and family members were provided by Dr. Öner Şanlı.

3.2. Chemicals

All chemicals used in this study were purchased from MERCK (Germany) or Sigma (USA), unless stated otherwise in the text.

3.3. Buffers and Solutions

3.3.1 DNA Extraction from Peripheral Blood

Cell Lysis Buffer	:	155 mM NH_4Cl, 10 mM $KHCO_3$ 0.1 mM Na_2EDTA (pH 7.4)
Nucleus Lysis Buffer	:	400 mM NaCl, 2 mM Na_2EDTA, 10 mM Tris (pH 8.2)
Proteinase K	:	20 mg/ml Proteinase K in dH_2O (Promega, USA)
Sodiumdodecylsulfate (SDS)	:	10 per cent SDS (w/v) in dH_2O
Ammonium Acetate	:	7.5 M CH_3COONH_4 in dH_2O

Ethanol	:	Absolute Ethanol (Carlo-Erba, Germany)
TE buffer	:	1 mM EDTA, 20 mM Tris-HCl, pH 8.0

3.3.2. Polymerase Chain Reaction (PCR)

10 X PCR Buffer	:	15 mM $MgCl_2$, 500 mM KCl, 100 mM Tris-HCl, pH 9.5 (Roche, Germany)
10 X PCR Buffer (Mg^{+2} free)	:	500 mM KCl 100 mM Tris-HCl (pH 8.3) (Roche, Germany)
10 X Guy's Buffer	:	166 mM $(NH_4)_2SO_4$, 67 mM $MgCl_2$, 1.7 mg/ml BSA, 670 mM Tris in TO.1E
TO.1E	:	0.1 mM EDTA, 20 mM Tris-HCl in dH_2O
$MgCl_2$	:	25 mM $MgCl_2$ (Promega, USA)
dNTP	:	12.5 Mm each of dATP, dCTP, dGTP and dTTP (Promega, USA) in dH_2O
DNA Polymerase	:	Promega (USA) and Roche (Germany)

3.3.3. Agarose Gel Electrophoresis

Agarose	:	2 per cent Agarose in 0.5 X TBE buffer
10 X TBE Buffer	:	20 mM EDTA, 0.89 M Boric Acid, 0.89 M Trizma base (pH 8.3)
10 X Loading Buffer	:	2.5 mg/ml Bromophenol Blue,

		1 per cent SDS in Glycerol
Ethidium Bromide	:	20 mg/ml in dH_2O

3.3.4. Denaturing Polyacrylamide Gel Electrophoresis (PAGE)

40 per cent Acrylamide (Stock)	:	40 per cent Acrylamide-bisacrylamide (19:1) in dH_2O
8 per cent Instagel	:	8 per cent Acrylamide-bisacrylamide (19:1), 8.3 M urea in 1 X TBE buffer
APS	:	10 per cent Ammonium Peroxidisulfate
TEMED	:	N,N,N,N-tetramethylethylenediamine
10X Loading Buffer	:	95 per cent Formamide, 20 mM EDTA, 0.05 per cent Xylene Cyanol, 0.05 per cent Bromophenol Blue

3.3.5. Single Strand Conformational Polymorphism (SSCP) Gel Electrophoresis

40 per cent Acrylamide (Stock)	:	40 per cent Acrylamide-bisacrylamide (37.5:1 or 50:1) in dH_2O
8 per cent Acrylamide (Non-denaturing)	:	8 per cent Acrylamide-bisacrylamide (37.5:1 or 50:1) in 0.6 X TBE buffer
Glycerol	:	5 per cent Glycerol in SSCP gel solution

3.3.6. Silver Staining

Staining Buffer (Buffer B)	:	0.1 per cent $AgNO_3$ (w/v) in dH_2O

Developing Buffer (Buffer C) : 1.5 per cent NaOH,
0.01 per cent $NaBH_4$,
0.015 per cent Formaldehyde in dH_2O

Stop Buffer (Buffer D) : 0.75 per cent $NaCO_3$ in dH_2O

Storage Buffer (Buffer E) : 5 per cent Glycerol in dH_2O

3.4. Fine Chemicals

3.4.1. Oligonucleotide Primers

A total of 27 oligonucleotide primer pairs were used in this study. These were either for microsatellite markers used in linkage analysis or for the exons of *SLC34A2*.

The oligonuclotide primers designed for amplification of the candidate gene SLC34A2 were purchased from GIBCO-BRL (USA). The lyophilized primers were dissolved in 100 µl dH_2O, and dilutions to 10 µM were used for PCR assays. The primers were designed to flank the exons and to amplify at least 13 nucleotides into the introns to enable the detection of mutations both in the exons and the conserved sequences around splice junctions. Primers for the largest exon (exon 13) were designed to produce 5 overlapping fragments in order to analyze the whole exon and part of the 3'UTR. The primer pair SLC34A2-13b did not yield efficient amplification; therefore, it was replaced by SLC34A2-13b.2. Since the first and second exons of *SLC34A2* were very close to each other, they were amplified together using a single primer pair. Another pair of primers was designed to amplify the 205-nucleotide region upstream of the first exon.

Primer design was carried out using the software Primer3, which is available at http://workbench.sdsc.edu. The sequences of the 21 primer pairs for analysis of exons are presented in Table 3.1. The primers indicated as 'Long' additionally refer to the sequencing primers for PAM family 1 patient.

Table 3.1. Primer sequences to amplify *SLC34A2* exons, flanking sequences and partial 3'UTR sequences.

Exon	Primer Name	Primer Sequence (5'-3')
2	SLC34 A2-5'ex2F	AGGGGAACCACAGAGGAAAT
	SLC34A2-5'ex2R	CTTTTATCAGGGGCAGTGGG
2 & 3	SLC34A2-2,3F	AGCCCAACCCCGATAAGTA
	SLC34A2-2,3R	ACCACAGGAAGTTTCCCTCC
4	SLC34A2-4F	ATGCCTTTCTCTCTCTCCCC
	SLC34A2-4R	TCAAGATAATGCCCCTCACC
	SLC34A2-4-longF	TTGCCAAACTTCTCAGGGTT
	SLC34A2-4-longR	CCTAAAACACTCCAGGAGGC
5	SLC34A2-5F	TCGATCACGTTGTGATTGTT
	SLC34A2-5R	TTCCCACCCTCAGATAGACA
	SLC34A2-5-longF	GCCTTGGATGGAGACTTCTG
	SLC34A2-5-longR	AAACACATTGTAGCTGGGGC
6	SLC34A2-6F	GGTAACTTTAGCCTGCCTCC
	SLC34A2-6R	CGTGGCCAAGAACAATAGAG
7	SLC34A2-7F	ACTAATCTGGCTGTCGGGGT
	SLC34A2-7R	GGGATGTTGTGGGTAGGAAG
8	SLC34A2-8F	CCCTGGGTTTGTGTCCTAAA
	SLC34A2-8R	GATTTTTCAGGGACTCCCAA
	SLC34A2-8-longF	TCTCCTTAGAGCCCCTCTCAC
	SLC34A2-8-longR	GATTTTTCAGGGACTCCCAA
9	SLC34A2-9F	AGTGTTGTGGGCATTTGTCA
	SLC34A2-9R	CGGATAAATAGGTCACCCCC
10	SLC34A2-10F	CATGCCCTCCTGACAAGATT
	SLC34A2-10R	GTGAGGCCTACAAGTGAGGG
11	SLC34A2-11F	GAGGCCATGACATCTCTTCC
	SLC34A2-11R	GGATGACAGGAAATGGCAGTG
12	SLC34A2-12F	ACTGCCATTTCCTGTCATCC
	SLC34A2-12R	AGTTTGCAAGACCATGGGTG
13	SLC34A2-5' 13F	TGGAATCCAGGTACCCTCTG
	SLC34A2-5' 13R	ATCAGGTAGAAGACGGCGAA
	SLC34A2-13aF	TCCAACCTCTTGTGTTGCAG
	SLC34A2-13aR	AGTCGGAGGCACAGTACCAG
	SLC34A2-13bF	CTGGTTGGTGTCGGGGTT
	SLC34A2-13bR	CTCCAAGTCCTCGCAGCA
	SLC34A2-13b.2F	GTTCCCGTCGTCTTCATCAT
	SLC34A2-13b.2R	CTCCTCCAAGTCCTCGCA
	SLC34A2-13cF	CTGTGTGACTGCCCCAAGT
	SLC34A2-13cR	ATCTCCTCGAGGTGGTGAAA
	SLC34A2-13c.for Pol.F	CAGAACTGGAACTTCCTGCC
	SLC34A2-13c.for Pol.R	ACCTCACCCTGAGCCTCTCT
	SLC34A2-3'-13F	AGAGAGGCTCAGGGTGAGGT
	SLC34A2-3'-13R	TTGGAATAAAAGTGCCCTGC

Fine mapping was performed with a total of 10 microsatellite markers, which were purchased from Iontek (Turkey) and Resgen. Iontek stock primers were diluted to 10 µM in 60 µl dH2O for PCR reactions. Resgen markers were purchased already at 20 µM concentration, and used as they were. The properties of microsatellite markers D4S2620,

D4S1533, D4S2953, D4S3013, D4S2948, D4S2941, D4S2305, D4S2397, D4S1609 and D4S1632 used in the fine mapping of the gene locus are given in Table 4.1.

3.4.2. Other Fine Chemicals

The PCR products to be sequenced were purified by using the QIAquick PCR Purification Kit (Qiagen, Germany). Deoxyribonucloside triphosphates (dNTPs) were purchased from Promega (USA). Taq DNA polymerase enzyme for PCR was purchased from Promega (USA) or Roche (Germany).

3.5. Equipment

Autoclave	:	Model MAC-601, Eyela (Japan) Prior-Clave (UK)
Balance	:	Electronic Balance, GecAvery (UK) BJ210C Precisa (Switzerland)
Centrifuges		:Centrifuge DuPont Instruments (USA) 5415C Eppendorf (Germany) Mini Spin Plus Eppendorf (Germany)
Deep Freezers	:	-20°C Bosch (Germany) -20°C AEG (Turkey) -70°C GFL (Germany)
Documentation System	:	BioDOC Video Documentation system Biometra (Germany) Gel Doc 2000 Bio-Rad (USA)
Electrophoretic Equipment	:	Horizon 58, Model 200 BRL (USA) Sequi-Gen Sequencing Cell Bio-Rad (USA) DCode Universal Mutation Detection

		System Bio-Rad (USA)
		Wide Mini Sub Cell Gt Bio-Rad (USA)
		Primo Minicell Thermo EC (USA)
Incubators		:Plus Series Gallenkamp (Germany)
		Orbital Gallenkamp (Germany)
Magnetic Stirrer	:	Hotplate Magnetic Stirrer, HS31
		Chiltern (UK)
		MR 3001 Heidolph (Germany)
Minishaker		:IB InterMed (Denmark)
		Rotamax Heidolph (Germany)
Power Supplies	:	Power Pac Model 3000 Bio-Rad (USA)
		Fotoforce 250 Fotodyne (USA)
Refrigerator	:	4°C Arçelik (Turkey)
Spectrophotometer	:	Lambda 3 UV/VIS Perkin-Elmer (USA)
Thermocyclers	:	MJ Research (USA)
		Techne Progene (UK)
		Thermal Reactor TR1 Hybaid (UK)
Transilluminators	:	Chromato-Vue Transilluminator,
		Model 1 TM-20UVP (USA)
		Fluorescent Table Consort (Belgium)
Vortex	:	Vortexmixer VM20 Chiltern Scientific (USA)
		REAX top Heidolph (Germany)
Waterbath	:	Water Bath D 3162
		Köttermann Labortechnik (Germany)

Water Purification System : Millipore Elix 3 Millipore (France)

3.6. Electronic Database Information

The database information of polymorphic markers for fine mapping of PAM locus was obtained from National Center for Biotechnology Information NCBI web site (http://www.ncbi.nlm.nih.gov).

The databases used to retrieve information on candidate genes were NCBI Map Viewer (http://www.ncbi.nih.gov/mapview) and NCBI Entrez Gene (http://www.ncbi.nih.gov/entrez /query.fcgi?db=gene), respectively.

The database used for gathering information about the disorders was Online Mendelian Inheritance in Man (http://www.ncbi.nlm.nih.gov/Omim).

The software used for designing primer pairs was PRIMER3 of The Biology WorkBench database (http:// workbench.sdsc. edu).

The database used for alignment of *Homo sapiens SLC34A2* with its homologs in other organism was NCBI Homologene.

The database used for blasting *Homo sapiens SLC34A2* sequence was NCBI Blast.

The internet site used for exonic splicing of the *Homo sapiens SLC34A2* was RESCUE-ESE web server (http://genes.mit.edu/burgelab/rescue-ese/).

4. METHODS

4.1. DNA Extraction from Peripheral Blood Samples

Genomic DNA from patients and their family members were isolated from peripheral blood samples. Ten ml of a peripheral blood sample from a subject was collected into a sterile vacutainer tube containing K_2EDTA as anticoagulant. The sample was transferred to a 50 ml falcon tube, and 30 ml of cold cell lysis buffer was added and mixed thoroughly. The mixture was kept at 4^oC for at least 15 minutes to allow lysis of plasma membrane. Leukocyte nuclei were collected by centrifugation at 5000 revolutions per minute (rpm) at 4^oC for 10 min. The supernatant containing cell debris was discarded, and the leukocyte nuclei in the pellet were washed by suspending in 10 ml cell lysis buffer and subsequent centrifugation for 10 min at 5000 rpm. The supernatant was discarded, and the nuclei were resuspended in 3 ml of nuclei lysis buffer by vortexing until all clumps dissolved. After the pellet had been resuspended fully, 80 µl of 10 per cent SDS and 50 µl of Proteinase K (20 mg/ml) were added and mixed gently by rotating the tube. The sample was incubated either at 56^oC for 3 hours (hr) or at 37^oC overnight to degrade the nuclear proteins. Protein residues were precipitated out by shaking vigorously after the addition of 1.7 ml of 9.5 M NH4Ac and subsequent centrifugation at 5000 rpm at room temperature for 25 min. The supernatant was transferred to a clean 50 ml Falcon tube. Two volumes of ethanol were added to precipitate out the DNA. After DNA threads became visible and collected at the surface, DNA was fished out carefully with a micropipette tip and transferred into a 1.5 ml Eppendorf tube. Residual ethanol was air-dried, and the DNA was dissolved in 500 µl of TE buffer and stored at -20°C.

4.2. Linkage analysis

The large PAM family had already been mapped roughly to chromosome 4p after a genome scan of the individuals 501, 503 and 504 with 156 autosomal microsatellite markers of the CHLC/Weber Human screening set version 8a, in our laboratory (Ninis et al., 2003). The data were confirmed in this study, and the locus was refined with additional markers at the locus. A total of 10 microsatellite markers were used in the linkage study. In

addition to the large family, three other PAM families and three unrelated PAM patients were investigated for linkage to the locus using six of the markers, namely, D4S1533, D4S2948, D4S2941, D4S2305, D4S2397 and D4S1632. However, TM patients were analyzed with only two of the markers, D4S2397 and D4S2941.

The extent of informativeness of the microsatellite markers was reported in the Research Genetics (Resgen) catalogue as heterozygosity observed in a study group. The properties of the markers (designation, average fragment size, optimum annealing temperature, repeat type and PCR buffer used) are presented in Table 4.1.

The genotyping data obtained from gene localization studies of the large PAM family was subjected to two-point and multi-point analyses flanked by markers D4S2620 and D4S1632. The other PAM families were not subjected to lod score analysis, since they were too small to yield significant information. Linkage analysis was performed under the assumption of autosomal recessive inheritance, full penetrance, a disease gene frequency of one in 100 000, parental consanguinity, equal recombination frequencies in both sexes and equal frequencies of marker alleles.

Ped-Check1.1 was used to detect Mendelian or genotyping errors in the linkage data. SimWalk2 version 2.91 was used for calculation of the multipoint lod score and construction of haplotypes, allowing minimum number of recombination events. The haplotypes for deceased individuals were deduced from those of sibs and children.

Table 4.1. Properties of markers used for fine mapping of the PAM locus

Marker	**Average Product Size (bp)**	**Repeat Type**	**Annealing Temperature (^{0}C)**	**Buffer Choice**
D4S2620	292	Tetra	57.5	Roche
D4S1533	188	Tetra	58	Roche
D4S2953	146	Di	55	Roche
D4S3013	154	Di	58	Roche
D4S2948	144	Di	58	Roche
D4S2941	164	Di	53.5	Roche
D4S2305	397	Tetra	49.5	Roche
D4S2397	135	Tri	54.5	Roche
D4S1609	170	Di	54	Roche plus 2.5 M betaine
D4S1632	276	Tetra	55	Roche

Two point lod scores for the disorder PAM was calculated using the MLINK program of the FASTLINK 4.1P package. Maximum lod scores and MLEs of recombination fractions were determined using the ILINK program of the same package. For the disorder analyzed, a fully penetrant autosomal recessive model of inheritance and a disease gene frequency of 0.00001 was assumed. The allele frequencies of each marker were set to be equal and depended on the number of alleles observed in the study.

DNA fragments that represented marker alleles were generated by polymerase chain reaction. PCR for each microsatellite marker was carried out in a total volume of 25 µl containing 1 X PCR buffer (with 1.5 mM Mg^{+2} final concentration), 300 nM of reverse and forward primer each, 0.2 mM of dNTP, 125 ng of genomic DNA, 0.2 U Taq DNA polymerase, and sufficient dH_2O to adjust the volume. After an initial denaturation step of 2 minutes at 95^0C, 35 cycles of 45 sec denaturation at 94^0C, 45 sec annealing at the optimal temperature, and 1 min elongation at 72^0C, and a final elongation step at 72^0C for 10 minutes were performed.

PCR products ready for allele determination were mixed with 10 X Stop solution in 1:1 ratio and kept at 4 ^{o}C until use. After incubating at 95^0C for 5 minutes for denaturation, they were loaded onto an 8 per cent denaturing polyacrylamide gel as described in sections 4.3.3 and 4.3.4. Alleles were resolved under constant power of 35 W for 1.5 to 3 hours and visualized by silver staining as described in Section 4.3.8.

4.3. Candidate Gene Approach

In this study, Single Strand Conformational Polymorphism (SSCP) was the starting mutation detection technique. 3'UTR, coding exons and flanking sequences were subjected to SSCP analysis followed by direct sequencing. SSCP technique is based on the fact that single stranded DNA under nondenaturing conditions assumes a unique secondary conformation that depends on the primary sequence. Thus, any single nucleotide change in the DNA sequence is expected to result in a conformational change that alters the migration pattern in an SSCP gel. However, the efficiency of the technique to detect mutations is estimated to be less than 100 per cent.

To confirm the presence of a potential nucleotide variation and to determine its nature, direct sequencing of the gene fragment in question was carried out. Sequence information allowed determining whether the nucleotide variation was likely to have any functional significance. A variant could lead to an amino acid substitution, affect the translational reading frame or cause aberrant splicing. It is also essential to investigate the frequency in the normal population of a variant identified. Hence, for all SSCP band shifts, population screening was performed to conclude that the variant was rare.

4.3.1. Amplification of the Candidate Gene by PCR

In order to analyze *SLC34A2* in the subjects in our study group, oligonucleotide primers were designed to amplify 3'UTR and coding exons and flanking sequences in the gene. PCR amplified fragments were analyzed by SSCP and, in case of PAM family 1 patients where no band-shift was observed, by direct sequencing. Primers were designed to generate DNA fragments shorter than 300 bp for optimal SSCP analysis except for SLC34A2-2,3 that was 359 bp long. In primer design, flanking intronic regions of the exons were taken into consideration as well, since they are known to play a role in the RNA splicing mechanism. 'Biology Workbench' was the program used for primer design. The sequences of the amplified regions of designed markers are given in Table 3.1.

PCR reactions were carried out in a total volume of 25 µl that contained 1 X PCR buffer, 0.2 mM of dNTP, 300 nM of a primer pair, 125 ng of genomic DNA, 0.2 U of Taq DNA polymerase, and sufficient dH_2O to complete the volume. Following an initial denaturation step of 2 minutes at 95^0C, 35 cycles of 30 sec denaturation at 94^0C, 30 sec annealing at the optimal temperature, and 2 min elongation at 72^0C and a final elongation step at 72^0C for 10 minutes were performed. PCR conditions optimized are presented in Table 4.2.

Table 4.2. PCR conditions for *SLC34A2* exons

Exon	Product Size (bp)	Annealing Temp. (^{0}C)	Buffer Choice
SLC34A2-5'ex2	300	59	Roche (2 mM Mg^{+2} end conc.)
SLC34A2-2,3	359	61.6	Roche (2 mM Mg^{+2} end conc.)
SLC34A2-4	216	62	Roche (3 mM Mg^{+2} end conc.)
SLC34A2-4-long	319	61.5	Roche (2 mM Mg^{+2} end conc.)
SLC34A2-5	256	64	Roche (2 mM Mg^{+2} end conc.)
SLC34A2-5-long	383	61.6	Roche (3 mM Mg^{+2} end conc.)
SLC34A2-6	231	59.9	Roche (3 mM Mg^{+2} end conc.)
SLC34A2-7	284	63.5	Roche (3 mM Mg^{+2} end conc.)
SLC34A2-8	211	59.9	Roche (2.5 mM Mg^{+2} end conc.)
SLC34A2-8-long	319	60.6	Roche (2 mM Mg^{+2} end conc.)
SLC34A2-9	219	58.2	Roche (2.5 mM Mg^{+2} end conc.)
SLC34A2-10	236	58.8	Roche (2 mM Mg^{+2} end conc.)
SLC34A2-11	204	61	Roche (2 mM Mg^{+2} end conc.)
SLC34A2-12	246	55	Roche (2.5 mM Mg^{+2} end conc.)
SLC34A2-5' 13	308	58	Roche (2 mM Mg^{+2} end conc.)
SLC34A2-13a	283	61.6	Roche (2 mM Mg^{+2} end conc., 8% DMSO)
SLC34A2-13b	285	53	Roche (2 mM Mg^{+2} end conc.)
SLC34A2-13b.2	273	61.6	Roche (2 mM Mg^{+2} end conc.)
SLC34A2-13c	277	57	Booster PCR, Roche (2 mM Mg^{+2} end conc.)
SLC34A2-13c.for Pol	272	62.2	Roche (2 mM Mg^{+2} end conc.)
SLC34A2-3' 13	249	58	Roche (2 mM Mg^{+2} end conc.)

4.3.2. Analysis of PCR Products on Agarose Gels

To visualize the extent of PCR amplification, a 5 µl aliquot of PCR product was mixed with 5 µl of 1 X loading buffer, loaded on a 2 per cent agarose gel containing 3 µg/ml Ethidium Bromide, and electrophoresed in 0.5 X TBE buffer at 175 volts for 7-10 minutes. DNA bands were subsequently visualized under a UV light transilluminator. To confirm the lengths of the PCR products and detect any nonspecific amplification, the products were further run on an 8 per cent denaturing gel as described in Section 4.3.3 and later visualized by silver staining as described in Section 4.3.8.

4.3.3. Preparation of Denaturing Polyacrylamide Gels

A polyacrylamide gel was cast in a 40 cm long sequencing apparatus that was assembled using 0.35 mm spacers. Thirty-five ml of 8 per cent denaturing Instagel was mixed with 300 µl of 10 per cent APS and 30 µl of TEMED to initiate and allow

polymerization. Immediately the gel was poured between the glass plates of the apparatus. Then a sharks-tooth comb that has the same thickness as the spacers was inserted in the inverted position between the glass plates. The gel was allowed to polymerize for at least one hour before electrophoresis.

4.3.4. Electrophoresis on Denaturing Polyacrylamide Gels

The polymerized gel was first run in preheated hot 1 X TBE buffer for about 15 min at a constant power of 45 W in order to allow the gel temperature to rise to 40-45^{0}C. This high temperature is essential to keep the DNA in its predenatured form. During the prerun, samples were prepared for loading by first mixing with 10 X Stop buffer in a 1:1 ratio, then denaturing at 95^{0}C for 4-5 minutes in a heat block or thermocycler and immediately chilling on ice.

Then, the comb was removed from the apparatus, and the upper part of the gel was cleaned from gel particles and urea by squirting electrophoresis buffer. Next, the comb was placed in the correct orientation to form loading slots. Depending on their band intensities on agarose gels, 3 to 6 µl of each sample was loaded into these slots. The gel was run at a constant power of 35 W for 1.5-3 hours to resolve the alleles. Finally, the gel was silver stained in order to visualize the fragments as explained in Section 4.3.8.

4.3.5. Single Strand Conformational Polymorphism Analysis

PCR products of PAM and TM patients from all families were analyzed for nucleotide variants in *SLC34A2* using SSCP technique. Whenever a mobility shift was observed, the fragment was analyzed similarly in several individuals to determine the frequency in the population. For a variant that was not obviously inactivating the gene, a population assay was carried out in at least 105 unrelated individuals, resulting in the analysis of an average of 127 total individuals for each such variant.

All variants including the possible mutants and polymorphisms were subjected to DNA sequence analysis to determine the nature of the variation. Since the efficiency of SSCP analysis is less than 100 per cent, PAM patients of the large family was subjected to

sequence analysis for all gene regions analyzed by SSCP, since they had not exhibited any pattern variation.

4.3.6. Preparation of SSCP Gels

The glass plates of the gel were 20 cm x 20 cm in size, and the apparatus was assembled using 0.75 mm spacers. Six ml of 40 per cent acrylamide stock was mixed with 1.8 ml of 10 X TBE, and the volume was adjusted to 30 ml by adding dH_2O. Polymerization of the gel was initiated by the addition of 300 µl of 10 per cent APS and 30 µl of TEMED. Immediately, the solution was mixed thoroughly and poured between the glass plates. A 20-well comb was inserted right after the gel was poured, and the gel was left to polymerize for at least an hour. After polymerization, the gel was cooled at 4^0C for at least half an hour before use.

4.3.7. SSCP Electrophoresis

Electrophoresis was carried out in 0.6 X TBE buffer at either 4^0C or 20^0C. Samples were mixed in 1:1 ratio with 10 X Stop buffer, denatured at 95^0C in a thermocycler for 5 min, and immediately placed on ice. Six µl of each sample was loaded and electrophoresed at a constant power of 6 W for 12-24 hours in the BioRad DCode Universal Mutation Detection System. Subsequently, in order to visualize the bands of the samples, the gel was silver stained as explained in Section 4.3.8.

4.3.8. Silver Staining

After electrophoresis was complete, the glass plates sandwiching the gel were removed from the apparatus and let cool down for a few minutes. The glass plates were separated very carefully so that the gel remained intact on one of the plates. The gel was very thin and prone to tearing, so a piece of filter paper was used to remove and support the adhering gel during transfer from the glass plate. The gel was placed in Buffer B together with the filter paper and shaken for 10-12 minutes. Buffer B was discarded, and the gel was washed briefly twice in dH_2O to remove excess silver. In the next step, the gel was incubated in Buffer C until bands appeared. Finally, Buffer C was discarded, Buffer D

was added, and the gel soaked in it for 10 minutes to terminate the staining reaction. For storage and documentation, the gel was transferred into a transparent folder with the aid of a paper towel to avoid tearing and folding.

4.3.9. DNA Sequence Analysis

As the first step, the DNA samples of interest were PCR amplified and the resulting PCR products purified. All samples including PAM patients, TM subjects and unrelated individuals from the population that exhibited variant SSCP patterns were subjected to direct sequence analysis using the same primers as in the SSCP analysis.

A DNA region to be sequenced was amplified in a 75 µl reaction and subsequently purified from the unused primers, dNTPs, and the genomic DNA by a QIAquick-spin column. First, 5X volume of buffer PB was added to the PCR product and mixed. The sample was then applied to a QIAquick-spin column placed in a 2 ml collector tube. The tube containing the mixture was centrifuged for 1 min at 13 rpm for DNA to enter the column and bind it. After discarding the flow-through, 750 µl buffer PE mixed with absolute ethanol in a 55 to 220 ratio was applied to the column to wash it. The washing step was completed by the centrifugation of the column for 1 min at 13 rpm to remove the buffer containing the primers and dNTPs. The last step was repeated to remove the residual buffer. The flow-through was discarded.

The column was placed into a sterile 1.5 ml microcentrifuge tube. Thirty to 50 µl of dH_2O was applied onto the column and left for 1 min. A final centrifugation of 1 min at the maximum speed facilitated the elution of DNA fragments with sizes 100 bp to 10 kbp. The purity of the eluted templates was checked on an 8% denaturing polyacrylamide gel.

Pure DNA fragments were later handed to Dr. Durişehvar Ünal in our department for sequence analysis. DNA sequencing instrument used was Amersham Biosciences ABI 310 Gene Analyzer.

5. RESULTS

In this study, positional-candidate gene approach was the strategy with linkage analysis forming the first part. In this respect, the candidate gene that is likely to be responsible for pulmonary alveolar microlithiasis was chosen after narrowing down the gene locus with linkage analysis. The data obtained were also supported by computerized analyses whenever it was necessary. In addition, Mapviewer tool of NCBI database (National Center for Biotechnology Information, http://www.ncbi.nlm.nih.gov/Mapviewer) was used to explore the genes within the identified locus. Then, the functions of those genes were considered in order to select the most plausible candidate gene that would be implicated in the etiology of the disease. Later, the candidate gene was subjected to mutation analysis.

5.1. Gene Localization

In the context of linkage studies, the locus for the autosomal recessive disorder PAM was refined by homozygosity mapping. The approximate gene locus that had been previously identified in our laboratory was confirmed and refined with more densely spaced markers. Later, the results obtained were subjected to computerized parametric lod score analyses. Both two-point and multi-point lod score tests were applied to the data generated.

5.1.1. Haplotype Analysis in Family 1

Pulmonary alveolar microlithiasis had been diagnosed in 6 members of a large consanguineous Anatolian family (Family 1, Şenyiğit et al., 2001). A genome scan in the three affected brothers of this family (namely, individuals 501, 503 and 504) had mapped the gene locus roughly to chromosome 4p in our laboratory. In the present study, the approximate interval was confirmed so that an identical genomic block was observed in the homozygous state in the patients and heterozygous state in their parents. Later, the gene locus was narrowed down to an 8.9 cM maximal interval at chromosome 4p15 using nine additional markers, namely, (tel) – D4S2620, D4S1533, D4S3013, D4S2948, D4S2941,

D4S2305, D4S2397, D4S1609 and D4S1632 – (cen). The pedigree of Family 1 and the deduced haplotypes with recombination events are given in Figure 5.1.

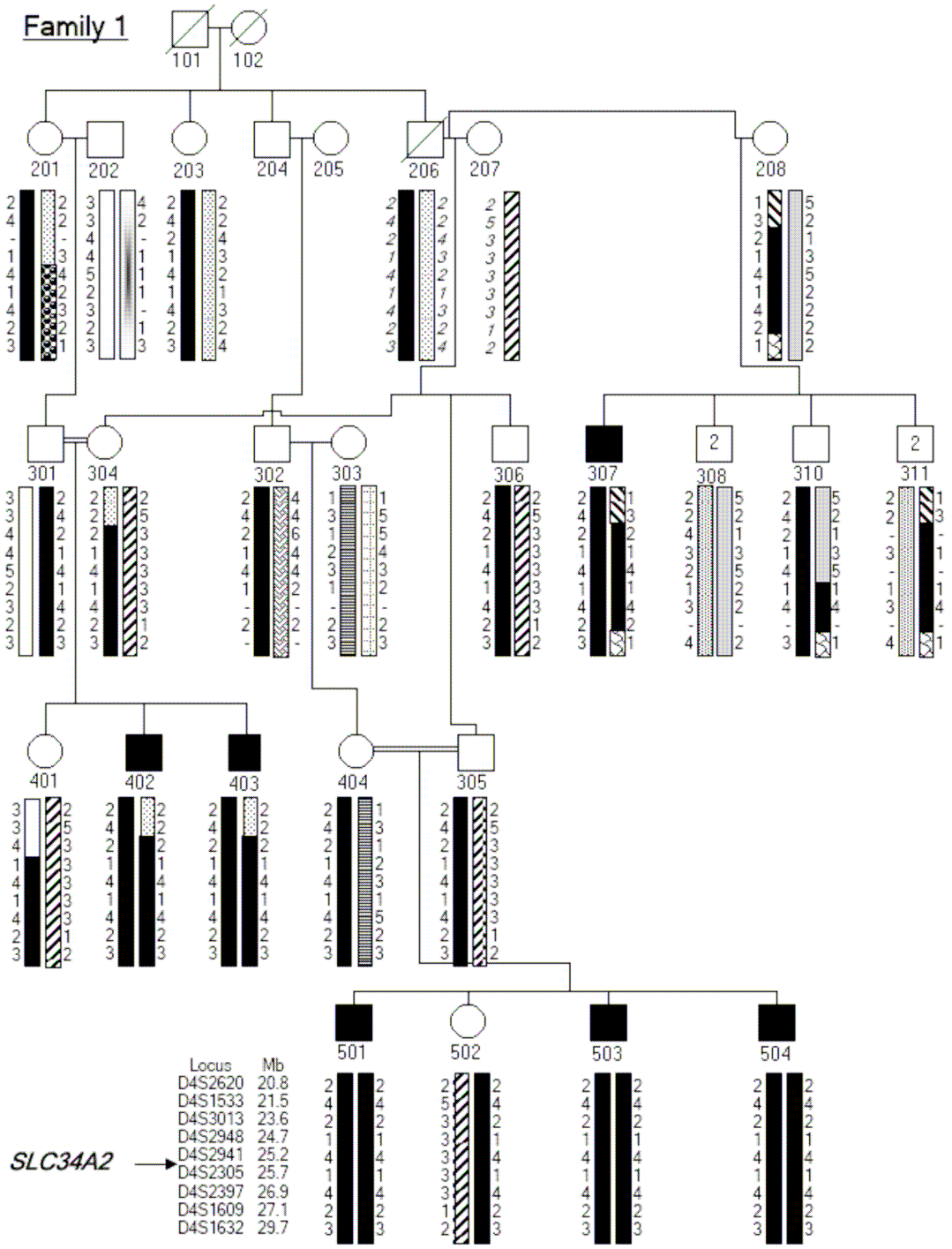

Figure 5.1. Pedigree diagram and haplotypes for 9 markers at 4p for Family 1.

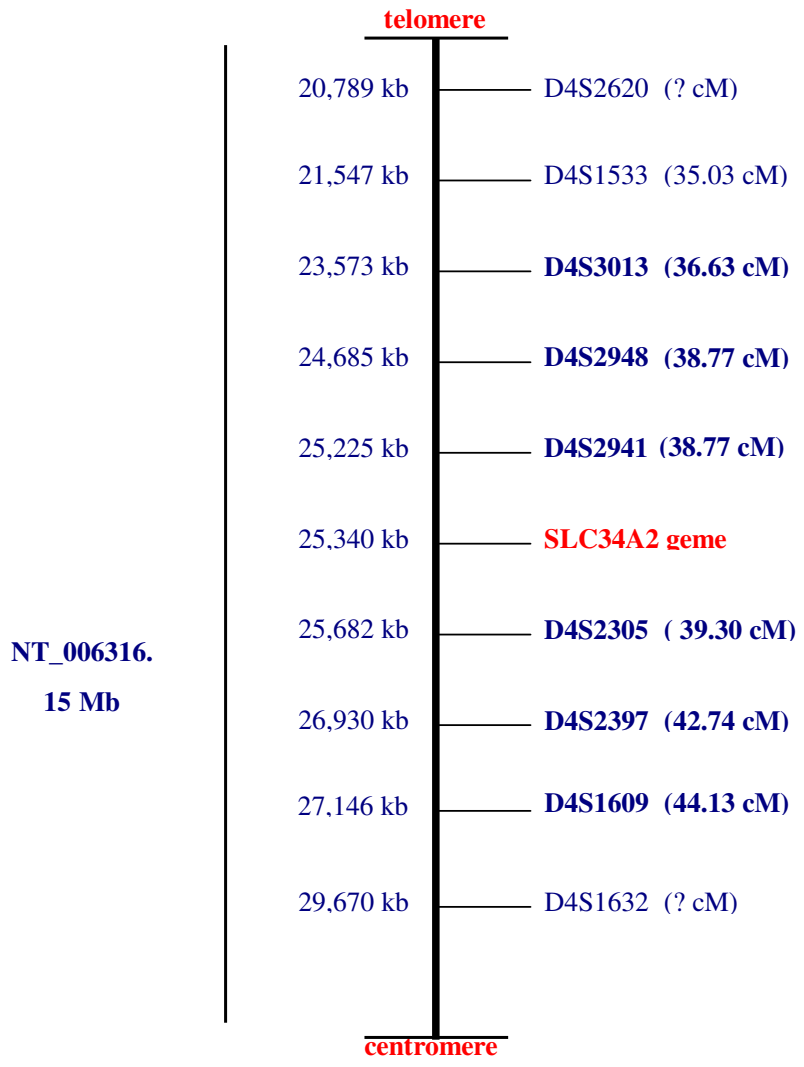

Figure 5.2. The map of markers and the candidate gene at the locus for PAM. Contig name and physical positions are given on the left in kb. Genetic positions are given on the right as cM from 4pter (Distances not to scale).

Haplotypes in italics in Figure 5.1 indicate that DNA was not available for analysis for those individuals but were deduced from the haplotypes of parents, sibs or children. Different haplotypes are shown by differentially shaded bars.

The maximum homozygosity region was found between markers D4S2620 and D4S1632 for the affected brothers 501, 503 and 504. The heterozygous state of patients 307, 402 and 403 for markers D4S2620 and D4S1533 narrowed down the PAM locus

telomerically, delineating the locus within D4S1533 and D4S1632. In addition, patient 307 was heterozygous for the centromeric boundary D4S1632.

Individual 310, who was carrying part of the identical homozygous block for markers D4S2305, D4S2397 and D4S1609 shared by affected subjects, was healthy. Therefore, this region of homozygosity was excluded from the gene locus.

As a result, minimum region of homozygosity for PAM locus was delineated by markers D4S2305 and D4S1533 corresponding to an interval of 4.2 Mb at chromosome 4p15.31-15.2. Figure 5.2 shows the relative physical and genetic positions of the markers and the candidate gene located in this region. Markers that are homozygous in all affected individuals of Family 1 are given in bold, and the stronge candidate gene is labeled in red.

Two-point and multi-point lod scores were calculated to assess the significance of the data.

5.1.2. Linkage Analysis

For TM, linkage analysis was performed with few markers as compared to PAM. Unlike PAM, DNA samples of only unrelated TM patients but no family members were available for homozygosity mapping. Therefore, two-point and multi-point linkage analyses could not be applied to TM subjects but only homozygosity was investigated.

Linkage analysis was performed to confirm linkage implied by the haplotype data. Two-point lod score analysis was performed using the marker data given in Figure 5.1. The maximum two-point lod score obtained was 5.15 at a recombination fraction of zero for marker D4S3013. Two-point lod scores for each marker versus the disease locus are presented in Table 5.1. Maximum lod scores for PAM and D4S3013, D4S2948 and D4S2941 were higher than the threshold value of 3 for accepting linkage.

Ten-point lod score analysis was performed using the 9 markers presented in Table 5.1 versus the disease gene locus. This resulted in a maximum lod score of 6 between

D4S3013 and D4S2305, placing the disease gene at a location starting from 23.6 Mb down to 25.7 Mb on the map given in Figure 5.3.

Table 5.1. Two-point lod scores between PAM and 9 markers at 4p

			Lod Score at θ =								
Locus	*Mb*	*cM*	*0*	*.001*	*.05*	*.1*	*.2*	*.3*	*.4*	Z_{max}	θ_{MLE}
D4S2620	20.8	-	-∞	1.00	1.45	1.43	1.13	0.76	0.39	1.47	0.07
D4S1533	21.5	35.03	-∞	3.13	3.49	3.34	2.69	1.85	0.93	3.48	0.05
D4S3013	23.6	36.63	5.15	5.06	4.68	4.19	3.14	2.03	0.93	5.15	0.00
D4S2948	24.7	38.77	5.12	5.02	4.63	4.13	3.06	1.92	0.77	5.12	0.00
D4S2941	25.2	38.77	4.71	4.62	4.23	3.74	2.75	1.77	0.86	4.71	0.00
D4S2305	25.7	39.30	2.59	2.54	2.32	2.05	1.49	0.97	0.49	2.59	0.00
D4S2397	26.9	42.74	-0.66	0.00	1.07	1.34	1.21	0.77	0.26	1.36	0.12
D4S1609	27.1	44.13	2.26	2.22	2.05	1.83	1.39	0.93	0.47	2.26	0.00
D4S1632	29.7	-	-∞	2.29	2.70	2.62	2.12	1.43	0.66	2.70	0.06

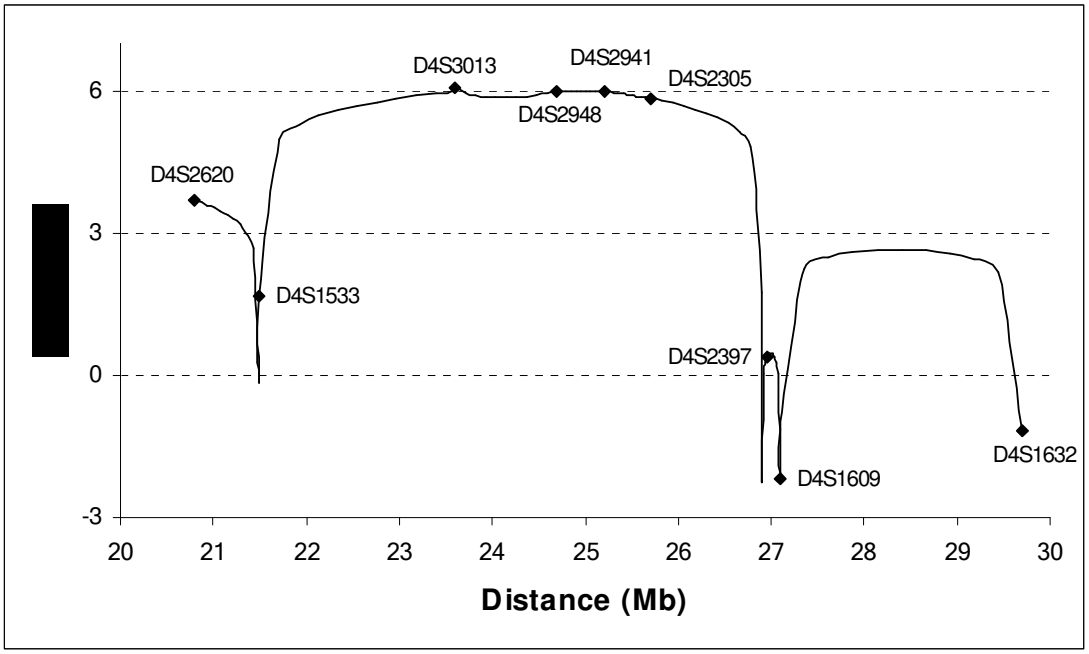

Figure 5.3. Multi-point linkage analysis at 4p15.31-p15.1 for Family 1. The microsatellite markers used in this study are plotted on the graph. The unit of x-axis is megabases of physical distance, and that for y-axis is lod score units.

5.1.3. Haplotype Analysis for PAM Subjects

Haplotypes of the members of Family 1 were presented in Figure 5.1. Besides those individuals, haplotypes for six other unrelated PAM patients were constructed to

investigate linkage to disease locus. For patients PAM25, PAM29 and PAM33, DNA samples from parents were also available. Table 5.2 presents those haplotypes.

Lod sore analysis was not applied to PAM subjects other than those in Family 1, because either the family sizes were too small for analysis or DNA sample of the parents were not available.

Marker alleles given in the above tables and figures were resolved on 8% denaturing polyacrylamide gels and visualized by silver nitrate staining. Examples of markers run on denaturing polyacrylamide gels are given in figures 5.4, 5.5 and 5.6.

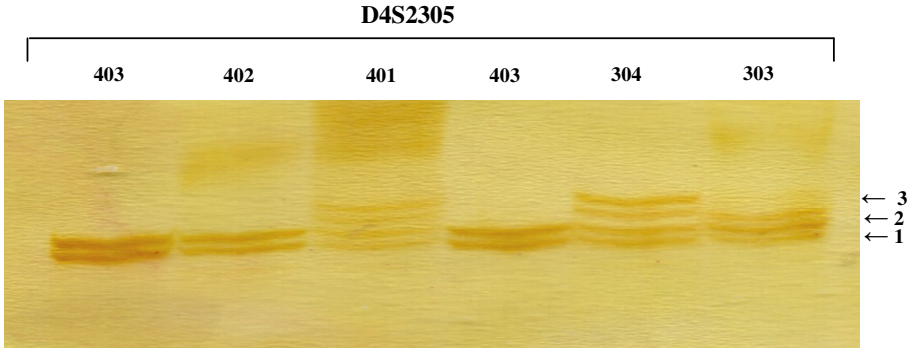

Figure 5.4. Silver-stained gel showing the genotypes of some of the Family 1 members for D4S2305. The numbers above are subject designations as in the pedigree and those on the right denote marker alleles.

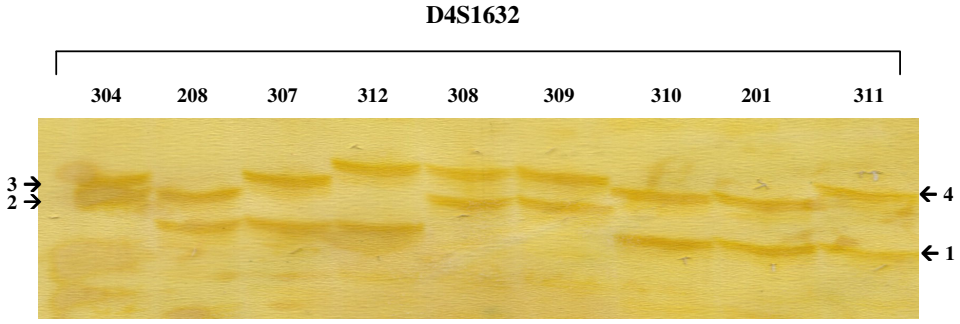

Figure 5.5. Silver-stained gel showing the genotypes of some members of Family 1 for D4S1632. The numbers above are subject designations and those on the right denote marker alleles.

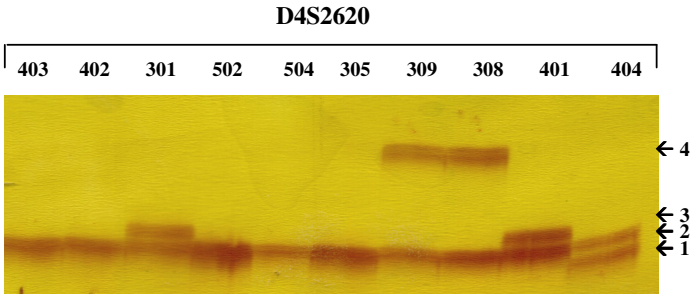

Figure 5.6. Silver-stained gel showing the genotypes of some members of Family 1 for D4S2620. The numbers above are subject designations and those on the right denote marker alleles.

5.1.4. Genotyping in TM Subjects

Testicular microlithiasis subjects were genotyped only for 2 markers that lie within the maximum region of homozygosity identified as PAM locus. Genome scan was not performed for these individuals, because TM was thought to be a complex disorder likely to result from defects in more than one gene. But since both PAM and TM are forms of microlithiasis, the candidate gene for PAM was thought to be at least partially responsible for TM as well. Single TM subjects were genotyped with D4S2397 and D4S2941. the genotypes are given in Table 5.3. Nevertheless, to investigate any homozygosity at the gene locus samples from all TM patients were run together on the same PAGE gels, using some of the Family 1 individuals as reference, so that the allele designations would be consistent among all PAM and TM subjects.

Table 5.2 and 3 as an excel document.

5.2. Candidate Gene Approach

The candidate gene SLC34A2 that was assessed to be responsible for PAM and perhaps for TM also, was analyzed for mutations in all TM and PAM individuals, including the healthy family members whenever available.

5.2.1. Gene Analysis in PAM Subjects

The gene locus identified contained 20 genes as reported in NCBI build 36.1. An evaluation of the genes pointed out a single candidate gene, namely *SLC34A2*. The gene stood out as the likely disease gene, since it was a phosphate transporter expressed strongly in lung.

Hence, *SLC34A2* was analyzed in the PAM patients by SSCP and subsequent DNA sequence analysis. All coding exons with flanking sequences and the 3'UTR were analyzed. Table 5.4 shows the flanking sequence lengths of each coding exon that are included in the PCR amplified fragments and thus subjected to SSCP and DNA sequencing. Forward primer of exon 2 and reverse primer of exon 3 were used together to amplify the two exons plus intron 2 as a single fragment. A similar procedure was applied to exons 10 and 11. Exon 13 was amplified as three overlapping fragments due to its long length. The frequency of any SSCP pattern variation in a healthy or affected individual was determined via population SSCP assay, and the variant was further identified at the nucleotide level by direct sequencing. All variants were screened in 7 unrelated PAM patients, 15 TM subjects and normal controls. Those that did not obviously inactivate the gene were screened in 105-123 normal controls, summing up to at least 210 chromosomes in total.

A total of five different homozygous mutations in all six unrelated PAM patients outside Family 1 were identified using both SSCP and sequencing. Table 5.5 shows the mutations and their predicted effects on translation and the protein product. All mutations were predicted to result in the loss of function of the protein. DNA mutation designations are based on cDNA, where +1 corresponds to ''A'' of the translational initiation codon ATG.

Table 5.4. The lengths of the flanking sequences of the coding exons included in the amplifications. A minus sign indicates the 5' site of the exon and a plus sign shows the 3' site of it.

5' site of the exon	Exon	3' site of the exon
- 185	2	+ 92 (whole intron 2)
- 92	3	+ 28
- 57	4	+ 93
- 72	5	+127
- 45	6	+ 34
- 13	7	+ 35
- 74	8	+ 108
- 14	9	+ 44
- 16	10	+ 12
- 13	11	+ 92 (whole intron 11)
- 38	12	+ 43
- 145	13	+ 189

Table 5.5. Novel *SLC34A2* sequence variants identified in PAM patients

Subject number	Mutation	Location	Effect on Translation	Predicted Consequence on Protein	Number of normal individuals carrying
PAM 24 & 29	c.114delA	Exon 3	Frameshift	Truncation	0 / 123
PAM 41	c.226C>T	Exon 3	p.Gln76X	Termination	0 / 123
PAM 33	c.316G>C	Exon 4	p.Gly106Arg	Substitution	0 / 123
PAM 23	c.1328delT	Exon 11	Frameshift	Truncation	0 / 74
PAM 25	c.1342delG	Exon 12	Frameshift	Truncation	0 / 36

The first homozygous mutation was the deletion of adenine at nucleotide +114 in exon 3 in PAM patients 24 and 29. Figure 5.7 shows the band shifts of these patients, on an SSCP gel. The frequency of this mutation c.114delA in the population is very low since it is seen only in two out of 6 PAM patients, 15 TM subjects and 123 unrelated controls.

Figure 5.8 shows the sequencing chromatograms of PAM patients 24 and 29 in comparison to a healthy control. 114delA results in a shift in the translational reading frame so that downstream codons are altered. The frameshift causes the generation of an early stop codon, seven codons downstream, leading to a truncated protein.

Another homozygous mutation in exon 3 was detected in PAM41. A cytosine to thymine conversion at nucleotide 226 of the CDS created a premature termination codon. SSCP results showed that PAM41 was the only individual carrying this mutation c.226C>T among all PAM and TM patients together with 123 healthy controls (Figure 5.7). Figure 5.9 shows the chromatograms of PAM41 and a healthy control.

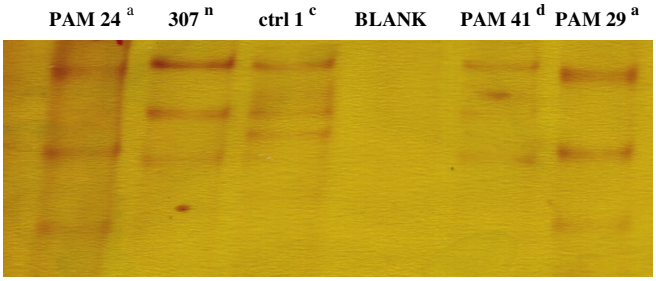

Figure 5.7. SSCP analysis of PAM 24 and PAM29. Each variant band pattern is indicated with a different letter. PAM41 is another variant that is discussed below. 307 is a normal control and control 1 carries a known polymorphism (dbSNP: 4697597).

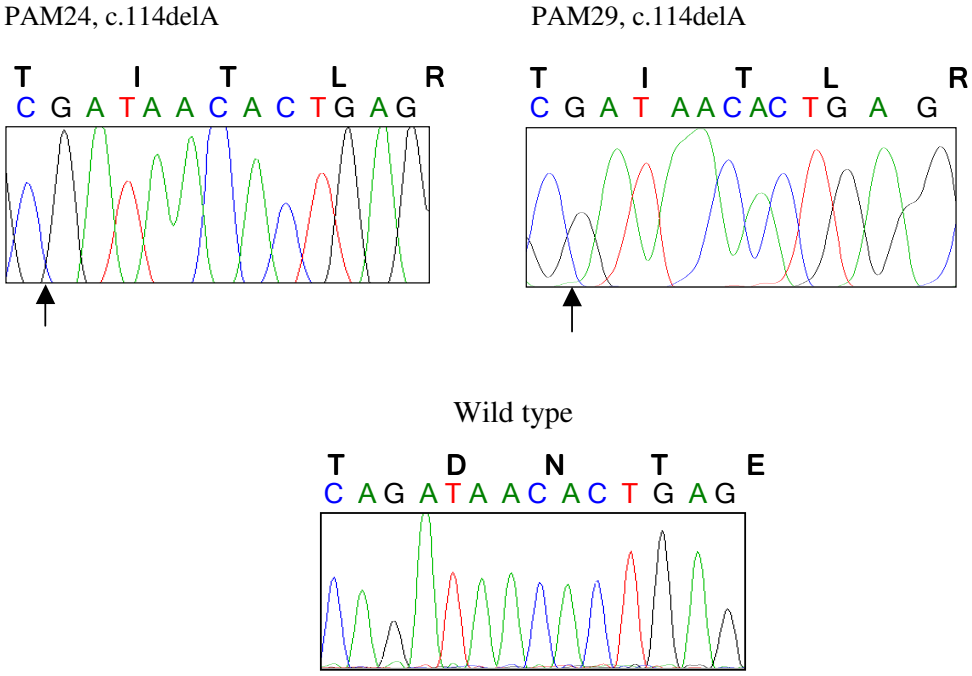

Figure 5.8. Chromatograms of the novel variant c.114delA in PAM24 and PAM29 and the corresponding sequence in a control. The capital letters above indicate the corresponding aminoacids and the arrow below the chromatograms show the site of the deletion.

In Figure 5.7, control 1 carries a known polymorphism (dbSNP: 4697597) of unknown frequency in NCBI database. Population SSCP among 123 normal controls in the present study shows that the frequency of this polymorphism is 20% in the normal population. Intersetingly, population SSCPs found out that DMD3.2 is a very rare variant from the population for the defined polymorphism dbSNP: 4697597. Because, unlike the other 123 individuals from the population, 7 PAM and 15 TM patients; the subject is homozygous for the guanine nucleotide at this position.

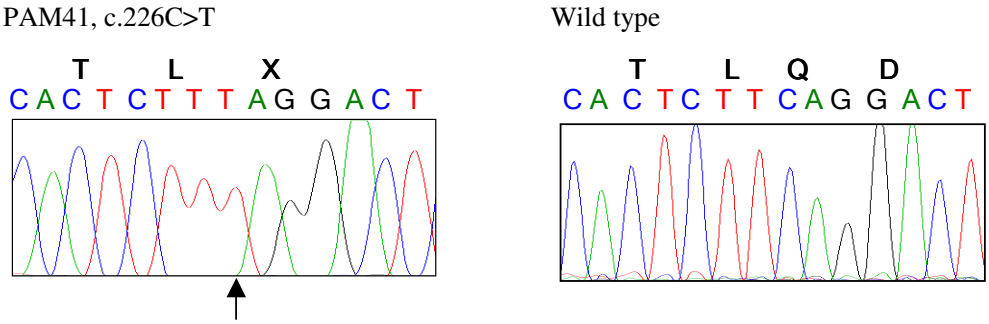

Figure 5.9. Chromatogram of the novel variant c.226C>T in PAM41 and the corresponding sequence in a control. The letter X above the chromatogram of the patient indicates translational termination due to a stop codon creation. The arrow below the chromatogram of the patient points out to the site of cytosine to thymine conversion.

Another homozygous mutation was in exon 4 of PAM33. It was a guanine to cytosine conversion at nucleotide 316 of the coding sequence, substituting arginine (designated R) for glycine (designated G), a basic aminoacid for a polar uncharged one. The glycine residue is conserved across species (chimpanzee, mouse, dog and chicken). This homozygous mutation c.316G>C was not found in the remaining PAM patients, 15 TM patients and 123 unrelated controls from the population; PAM33 was the only individual showing that particular SSCP pattern on the gel (Figure 5.10). Figure 5.11 shows the chromatograms of PAM33 and a healthy control. The arrow shows the position of the substitution.

In PAM patient 23, a homozygous deletion of a thymine at nucleotide 1328 of CDS was observed in exon 11. The resulting deletion led to a shift of the translational reading frame and predictably to the truncation of the protein. This mutation c.1328delT was not

observed in other PAM or TM patients or in 74 individuals in the population (Figure 5.12). Figure 5.13 shows the chromatograms of PAM23 and a normal individual.

PAM patient 25 was found to carry a homozygous mutation at nucleotide 1342 of the CDS which was an exonic deletion in exon 12. The deletion of the guanine nucleotide at this position resulted in a frameshift, creating a premature termination codon and leading to the truncation of the protein. This mutation c.1342delG was not seen in other PAM or TM individuals, nor in the 36 individuals from the population. The SSCP band shift of the mutation is shown in figure 5.14. Also, figure 5.15 shows the chromatograms of the PAM patient 25 and a healthy control.

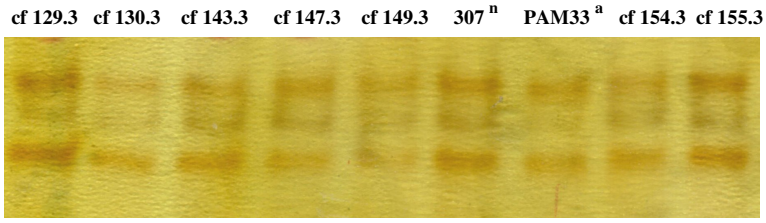

Figure 5.10. SSCP analysis of PAM33. The slightly different SSCP pattern of PAM33 together with the normal control (n) 307 from Family 1 and unrelated individuals from the population are shown.

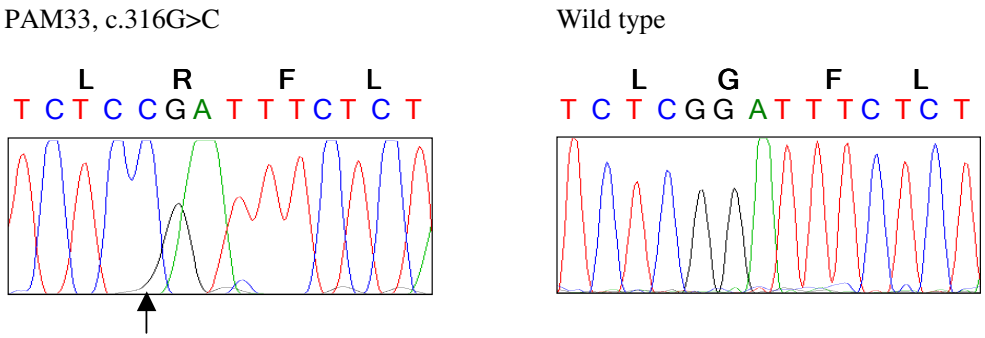

Figure 5.11. Chromatogram of the novel variant in PAM33 and the corresponding sequence in a control. The arrow below the chromatogram of the patient denotes the site of transversion.

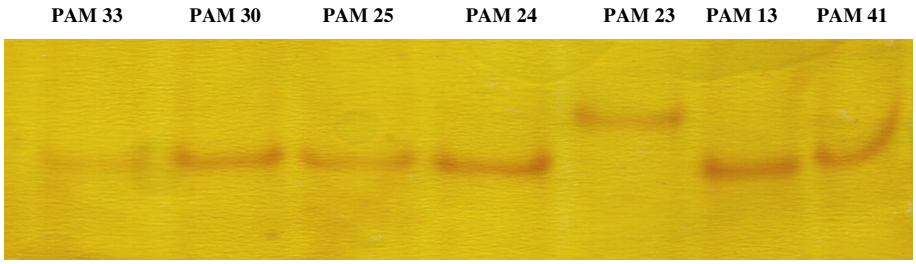

Figure 5.12. PAM 23 showing a different SSCP pattern among all PAM patients.

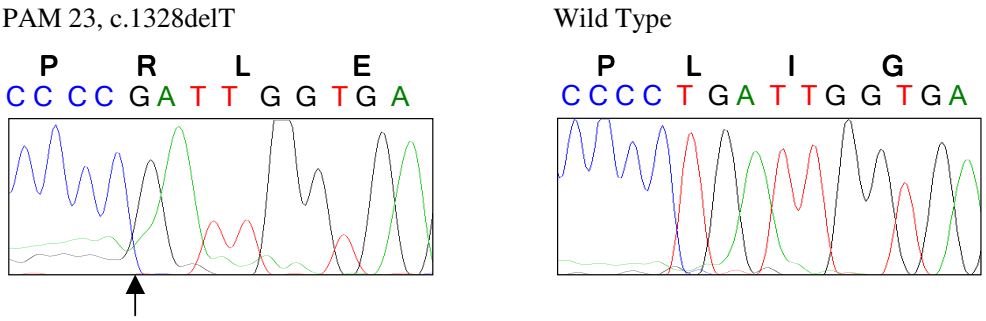

Figure 5.13. Chromatogram of the novel variant in PAM23 together with the corresponding sequence in the control. The arrow points out to the position of deletion.

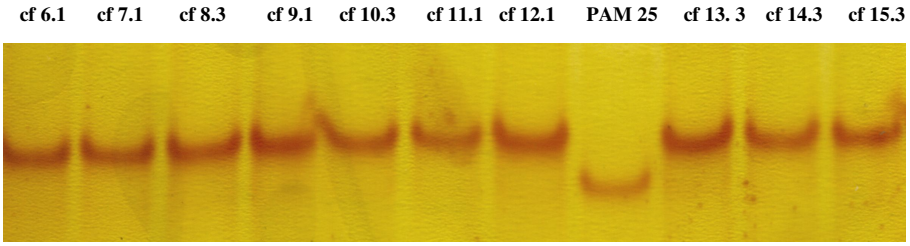

Figure 5.14. The different SSCP pattern of PAM25 and unrelated individuals from population.

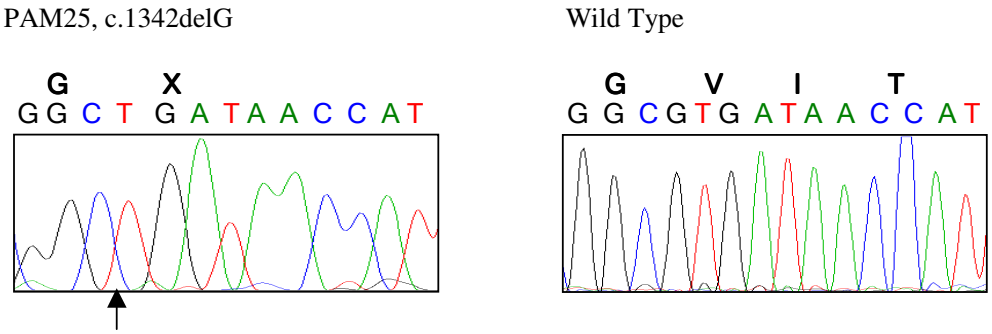

Figure 5.15. Chromatogram of the novel variation c.1342delG in PAM25 and the corresponding sequence in a control. The arrow indicates the site of deletion.

There were a total of seven PAM patients in the study. The mutations were identified in all patients except for that of Family 1. When we consider the fact that linkage to *SLC34A2* locus was performed with Family 1, it is very interesting not to find the mutation in this family. Besides SSCP analysis, direct DNA sequencing was carried out for all the coding exons of the gene for the family patients, but no variation was detected. The flanking sequence lengths of each coding exon that are subjected to SSCP and DNA sequencing is given in Table 5.4.

5.2.2. Gene Analysis in TM Subjects

Moderate expression of *SLC34A2* in testis prompted us to search for mutations in men with diffuse bilateral TM. In this part of the study, all coding exons of the gene were analyzed in the TM patients by SSCP. All coding exons with flanking sequences and the 3'UTR were studied, as was done for PAM patients (Table 5.6.).

Two variations, one being rare, were identified in the heterozygous state in two of the 15 TM subjects studied by SSCP (table 5.7). The variants were further studied at the nucleotide level by direct sequencing.

Table 5.6. Exons and lengths of their flanking introns that were analyzed by SSCP.

5' site of the exon	Exon	3' site of the exon
- 185	2	+ 92 (whole intron 2)
- 92	3	+ 28
- 57	4	+ 93
- 39	5	+46
- 45	6	+ 34
- 13	7	+ 35
- 47	8	+ 28
- 14	9	+ 44
- 16	10	+ 12
- 13	11	+ 92 (whole intron 11)
- 38	12	+ 43
- 145	13	+ 189

The first heterozygous variant was in TM4, a synonymous T to C conversion in exon 6 at nucleotide 552 of the CDS c.[=,552T>C(p.-)]. Although the nucleotide residue has been conserved in chimpanzee, interestingly it is a C in mouse, dog and chicken. It

created a hexamer proposed to be an exonic splicing enhancer that plays an important role in constitutive or alternative splicing. Figure 5.16 shows the SSCP pattern of TM4. Also, figure 5.17 shows the sequencing chromatogram of the TM patient and a healthy control for comparison. The variant is not very rare, since population SSCPs showed that two unrelated individuals from the population carried it. So there were three individuals with this heterozygous pattern among 7 unrelated PAM patients, 15 TM subjects and 108 normal controls.

Table 5.7. Novel *SLC34A2* sequence variants identified in TM subjects.

Subject Number	Mutation	Location	Effect On Translation	Predicted Consequence on Protein	Number of normal individuals carrying
TM4	c.[=,552T>C(p.-)]	Exon 6	p.Ile184Ile	Aberrant splicing	2 / 108
TM6	*[=,27G>T]	3'UTR	Not known	Not known	0 / 105

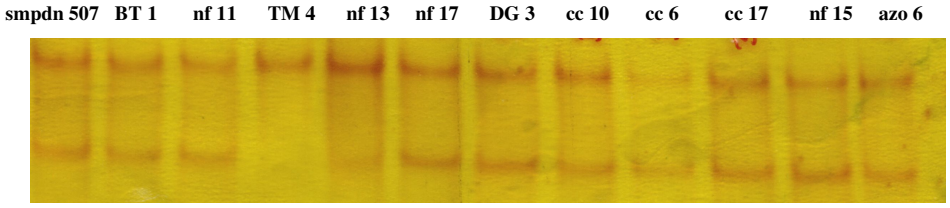

Figure 5.16. The SSCP pattern variant in TM4 and unrelated individuals from the population. Unlike the other individuals with a single band, TM4 has two bands.

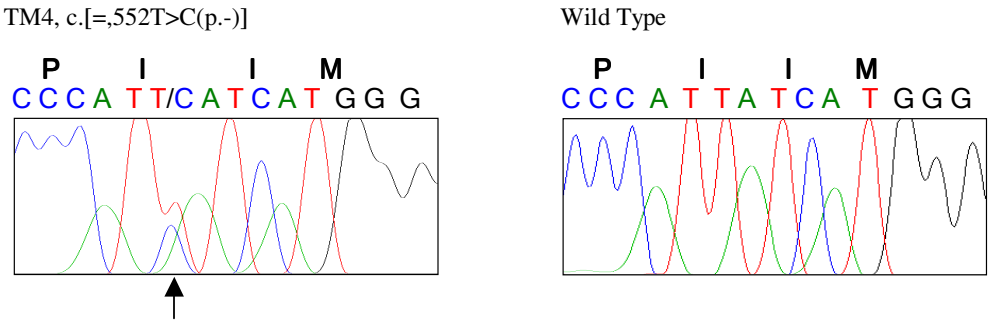

Figure 5.17. Chromatogram of the novel variant c.[=,552T>C(p.-)] in TM4 and the corresponding sequence in a control. The arrow indicates the site of heterozygosity.

The second heterozgous variant was in TM6, a G to T transversion 27 nucleotides downstream of the termination codon. SSCP analysis among 105 normal controls, 15 TM

and 7 PAM patients showed that TM6 was the only individual carrying the variant. This non-coding residue ∗[=,27G>T] is conserved in chimpanzee; however, the sequences downstream of termination are not conserved at all among other species. Figure 5.18 contains the chromatogram of the patient in addition to a healthy control.

While analyzing PAM and TM patients by SSCP technique, a rare variant was detected in an unaffected female in the control group. The identified novel variant c.[=,989C>T] of N30 was shown to carry a cytosine to thymine transversion in a single gene copy. In order to detect the frequency of this variant, a total of 106 unrelated controls from the population were analyzed in addition to 7 PAM and 15 TM patients. Population SSCP (Figure 5.19) showed that N30 was the only individual carrying the change. Figure 5.20 contains the chromatogram of the rare variant in N30 in comparison to a negative control from the population.

As a result of the transversion c.[=,989C>T] , threonine is substituted by methionine (a polar one by a non-polar) , most likely inactivating the protein. The residue has been conserved in chimpanzee and mouse but substituted with serine in dog and chicken.

TM6, ∗[=,27G>T]

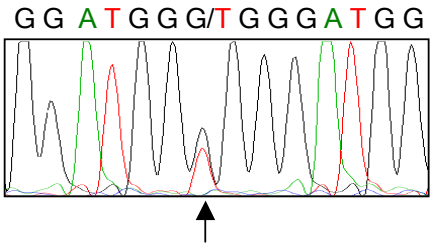

Wild Type (dbSNP: 3733545)

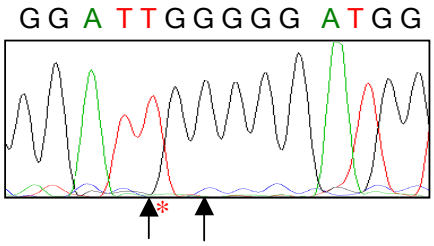

Figure 5.18. Chromatogram of the novel variant ∗[=,27G>T] in TM6 and the corresponding sequence in a control. In the wild type control, the arrow on the left* shows a reported polymorphism two nucleotides upstream with its SNP number indicated above the chromatogram.

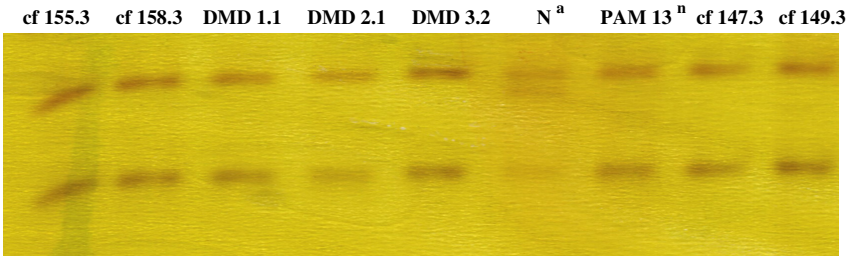

Figure 5.19. The SSCP pattern variant of N30 and unrelated individuals from population together with PAM13 used as negative control. Unlike the other individuals with two bands, N30 has three bands.

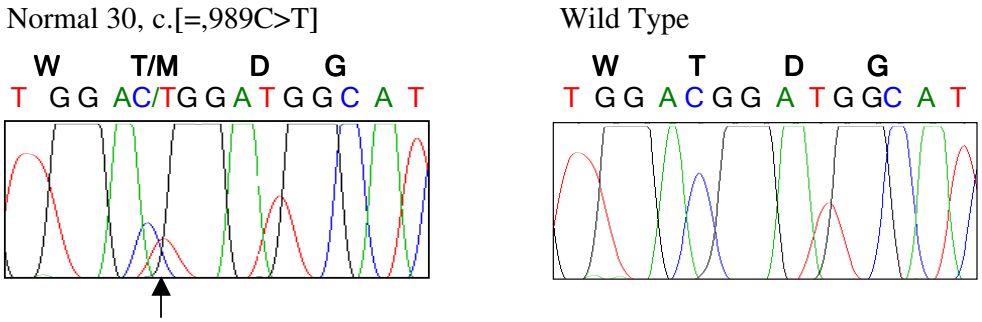

Figure 5.20. Chromatogram of the novel variant c.[=,989C>T] and the corresponding sequence in a control. The arrow indicates the site of heterozygousity.

6. DISCUSSION

In this study, we aimed to identify the gene responsible for PAM, a recessive disorder. It was assumed that the gene locus was homozygous and the disease alleles identical by descent as a result of consanguinity in the patients we studied. A large consanguineous family provided the genetic material for the linkage study, since it was essential to find two or more patients having a common chromosomal region within the disease locus to narrow it down and obtain a high cumulative lod score.

A total of 9 consecutive microsatellite markers were employed to confirm the previously identified disease locus. This locus at chromosome 4p15.31-15.2 was narrowed down to a 4.2 Mbp interval flanked by markers D4S1533 and D4S2305. The two-point and ten-point lod scores yielded very high values, 5.15 and 6, respectively, confirming the identification of the locus.

The genes that lied within the refined locus were identified through a database search. Only one candidate gene, *SLC34A2*, among the 20 genes at the locus stood out as the likely disease gene, since it was a phosphate transporter expressed strongly in lung. *SLC34A2* is a member of the solute carrier family SLC34A that plays a major role in the inorganic phosphate homeostasis and is expressed most strongly in fetal and adult lung. It has been suggested, therefore, to play an important physiological function in lung.

All twelve coding exons of *SLC34A2* were analyzed in PAM patients by SSCP and subsequent DNA sequence analysis for variants. Five different homozygous mutations were detected in six unrelated PAM patients outside the large family. Three of the mutations were frameshifts, one was a chain termination, and the final one was an amino acid substitution. Since the loss of function of the protein product of the gene could be compatible with calcium phosphate deposition in lung, the mutations found seemed to be consistent enough to blame a defected *SLC34A2* for PAM.

The mutation affecting the large family could not be found. All coding exons as well as introns 2, 11 and 3’ UTR of the gene were subjected to direct sequence analysis.

No mutation within these regions was detected, indicating the mutation was in exon 1, other introns or the promoter. Such a mutation could affect translation initiation, the proper functioning of an enhancer or silencer, or create a novel splicing site that would disrupt proper splicing of the transcript. The next step for this part of the study would be to find the mutation in the large family via SSCP and direct sequencing analyses of the non-coding exon, introns and promoter.

Phosphate is part of the surfactant in alveoli (Traebert et al., 1999). SLC34A2 gene is believed to uptake phosphate that has leaked into the alveolar space. This is in agreement with our results that phosphate uptake in lung is performed mainly by this gene's protein product.

Our findings showed that PAM was certainly a recessively inherited disease that was not caused by environmental factors. As none of the healthy members of the large PAM family was homozygous for the disease haplotype, it is certain also that the disorder is fully penetrant. Turkey is the country where the highest incidence of the disease has been reported. However, there were no common mutations carried by the unrelated patients to indicate the presence of a mutation prevalent in the population. Only PAM24 and PAM29 shared the same mutation. Since their families originated from different parts of the country, it is more likely that the mutation was not identical by descent but a recurrent one. It is now obvious that the high incidence of the disease in Turkey is due to the high frequency of consanguineous marriages, since the mutations in all PAM patients were homozygous. However, the haplotypes of all patients other than family 1 are not homozygous for all studied markers close to the gene locus. D4S2941 interrupts the region of homozygosity around *SLC34A2* in patients PAM24, PAM25, PAM29 and PAM41. As database errors occur often, this heterozygous marker interrupting the homozygous region may be hypothesized as misplaced in the genome database. It is very unlikely that a double-crossover occurred in this small interrupting region, which could explain occurrence of a heterozygous marker within a homozygous block. Therefore, the order of the marker is not convincing. Alternatively, the analysis might be incorrect in that, a site other than the marker locus would have been amplified.

The microliths that are known to form in the course of PAM had been shown to be composed of calcium phosphate deposits (Pracyk et al., 1996, De Jong et al., 2004). Until now, calcium ions have been blamed for the pathogenesis of PAM. However, our findings show that it is phosphate that is responsible, most likely forming microliths by chelating calcium ions in the extracellular fluid of lung.

As microliths from both PAM and TM subjects had been found to be composed of calcium and phosphate and there is moderate expression of *SLC34A2* in testis, we also searched for mutations in 15 men with diffuse bilateral TM in order to detect any possible effect of the gene on TM. For this purpose, SSCP was performed, and two rare variants were identified by subsequent DNA analyses. However, the change was either silent at the protein level or it was in the 3'UTR, making it difficult to assign with certainty these variants as mutations. Any possible effect of these changes on the expression of the gene or on its protein product must be further studied.

The first variant TM4 formed a hexamer that was proposed to be an exonic splicing enhancer playing an important role in splicing of the pre-mRNA (Fairbrother et al., 2002, Yeo et al., 2004). Alternative splicing could decrease the number of full transcripts in the cell, lowering the activity of the gene.

The second variant TM6 is a nucleotide substitution in a residue conserved in chimpanzee. However, the sequences downstream of the translational termination codon have not been conserved at all among other species. The variant's effect on the conformation of the mRNA was analysed using programRNA2, but supportive results were not obtained. Therefore, a possible effect of this variant on mRNA stability could not be found. But, since the change is seen only in this subject among a total of 127 individuals, it is obvious that the variant is very rare. So, studies on the mRNA and protein levels must be carried to define a probable effect of the variant on the expression level of the gene.

The reason why we found only two TM variants could be due to the low efficiency of the SSCP technique, hence, some of the TM variants may have escaped detection. In order to increase the mutation detection rate of SSCP, different gel systems, including polyacrylamide gels with 2 or 2.6 per cent cross-linking ratios or 0.5 X MDE gels, all with

or without glycerol, could be applied. Also, the variants may be located in non-coding regions of the gene not analysed in this study. It should also be noted that unlike PAM, TM is expected to be a complex disorder that may result from the mis-functioning of more than one gene. Thus, it is also probable that most TM patients carry no *SLC34A2* variants or the variants they show may be heterozygous as in the case of the two variants observed in the present study.

As the *SLC34A2* gene is also expressed in kidney, pancreas, prostate, ovary, small intestine, mammary gland, liver and placenta, which are organs that are known to exhibit idiopatic calcifications, it can be proposed that mutations in *SLC34A2* can at least be partially responsible for these calcifications. This proposal is further supported by the knowledge that, in some PAM patients, calcium deposits are observed in additional organs like pleura, kidneys, seminal vesicles, urethra and gall bladder. It would especially be interesting to study mammary calcifications since the malignant forms of them are known to contain calcium phosphate (Frappart et al., 1984).

Now that the gene responsible for PAM has been identified, it may be possible to develop gene therapy for the disease. Also, individuals at risk can be screened for mutations in *SLC34A2*, allowing early diagnosis of PAM. Similarly, prenatal genetic testing can be performed.

REFERENCES

Aizenstein, R. I., J. F. Hibbeln, B. Sagireddy, A. C. Wilbur and H. K. O'Neil, 1997, "Klinefelter's syndrome associated with testicular microlithiasis and mediastinal germ-cell neoplasm", *Journal of Clinical Ultrasound*, Vol. 25, pp. 508–510.

Arslan, A., T. Yalin, H. Akan and U. Belet, 1996, "Pulmonary alveolar microlithiasis associated with calcifications in the seminal vesicles", *Journal Belge de Radiology*, Vol. 79, pp. 118-119.

Başaran, N., S. Saylı, A. Başaran, M. Solak, S. Artan and J. Stevenson, 1998, "Consanguineous Marriages in the Turkish Population", *Clinical Genetics*, Vol. 34, pp. 339-341.

Bennett, H. F., W. D. Middleton, A. D. Bullock and S. A. Teefey, 2001, "Testicular microlithiasis: US follow–up, *Radiology*", Vol. 218, pp. 359–363.

Biary, M. S., M. A. Abdullah, H. M. Assaf and A. Wazzan, 1993, "Pulmonary Alveolar Microlithiasis in a Saudi child and two cousins", *Annals of Tropical Paediatrics*, Vol. 13, pp. 409-413.

Bieger, R. C., E. Passarge and A. J. McAdams, 1965, "Testicular intratubular bodies", *Journal of Clinical Endocrinology*, Vol. 25, pp. 1340–1346.

Bogart, S. D., 1980, "Disseminated pulmonary calcinosis with pulmonary alveolar microlithiasis", *NY State Journal of Medicine*, Vol. 80, pp. 1283-1284.

Burguet, W., A Reginster, 1967, "L'hérédité de la microlithiase alvéolaire pulmonaire: A propus d'une nouvelle observation familiale", *Ann Génét*, Vol. 10, pp. 75-81.

Bushby, L. H., F. NAC. Miller, S. Rosairo, J. L. Clarke and P. S. Sidhu, 2002, "Scrotal calcification: Ultrasound appearances and distribution", *Br J Radiology*.

Castellana, G., M. Gentile, R. Castellana, P. Fioren and V. Lamorgese, 2002, "Pulmonary Alveolar Microlithiasis: Clinical Features, Evolution of the Phenotype, and Review of the Literature", *American Journal of Human Genetics*, Vol. 111, pp. 220-224.

Castellana, G., and Vito Lamorgese, 2003, "Pulmonary Alveolar Microlithiasis: World Cases and Review of the Literaure", *Respiration*, Vol. 70, pp. 549-555.

Cluzel, P., P. Grenier, P. Bernadac, F. Laurent and J. D. Picard, 1991, "Pulmonary Alveolar Microlithiasis: CT findings", *Journal of Computer Assisted Tomography*, Vol. 15, pp. 938-942.

Coetzee, T., 1970, "Pulmonary alveolar microlithiasis with involvement of the sympathetic nervous system and gonads", *Thorax*, Vol. 25, pp. 637-642.

De Jong, B. W., C. A. De Gouveia Brazao, H. Stoop, K. P. Wolffenbuttel, J. W. Oosterhuis, G. J. Puppels, R. F. Weber, L. H. Looijenga, D. J. Kok, 2004, "Spectroscopic analysis identifies testicular microlithiasis as intratubular hydroxyapatite", *Journal of Urology*, Vol. 171, pp. 92-96.

Doherty, F. J., T. L. Mullins, G. R. Sant, M. A. Drinkwater and A. A. Ucci, 1987, "Testicular microlithiasis, A unique sonographic appearance", *JUltrasound in Med*, Vol. 6, pp. 389–392.

Enacar, N., S. Yavuzer, B. S. Sayli, G. Karabiyikoglu and N. Ekim, 1978, "Pulmoner Alveolar Mikrolityazis", *Tuberkuloz ve Toraks*, Vol. 26, pp. 186-196.

Fairbrother, W. G., R. F. Yeh, P. A. Sharp, C. B. Burge, 2002, "Predictive identification of exonic splicing enhancers in human genes", *Science*, Vol. 297, pp. 1007-1013.

Felson, B., 1988, "Chest Roentgenology", *1st ed. India, W. B. Saumders Company*, pp. 419.

Frappart, L., M. Boudeulle, J. Boumendil, H. C. Lin, I. Martinon, C. Palayer, Y. Mallet-Guy, 1984, "Structure and composition of microcalcifications in benign and malignant lesions of the breast: study by light microscopy, transmission and scanning electron microscopy, microprobe analysis, and X-ray diffraction", *Human Pathology*, Vol. 15, pp. 880-889.

Ganem, J. P., K. R. Workman and S. F. Shaban, 1999, "Testicular microlithiasis is associated with testicular pathology", *Urology*, Vol. 53, pp. 209–213.

Hilfiker, H., O. Hauenhauer, M. Traebert, L. Forster, H. Murer and J. Biber, 1998, "Characterization of a new murine type II sodium-phosphate cotransporter expressed in mammalian small intestine", *Proc Natl Acad Sci USA*, Vol. 95 pp. 14564–14569.

Janzen, D. L., J. R. Mathieson and J. I. Marsh, 1992, "Testicular microlithiasis: Sonographic and clinical features", *American Journal of Roentgenology*, Vol. 158, pp. 1057–1060.

Jaramillo, D., A. Perez-Atayde and R. L. Teele, 1989, "Sonography of testicular microlithiasis", *Urolog Radiology*, Vol. 11, pp. 55–57.

Khan, M. A., B. Beyzade and B. S. Potluri, 2000, "Testicular seminoma in a man with bilateral microlithiasis and a history of cryptorchidism", *Scand J Urol Nephrol*, Vol. 34, pp. 377–379.

Lander, E. S. and D.Botstein, 1987, "Homozygosity Mapping: A Way to Map Human Recessive Traits with the DNA of Inbred Children", *Science* , Vol. 236, pp. 1567-1570.

Leman, J., J. P. Brush and M. J. Tidman, 2000, "Multiple lentigines and microlithiasis", *Clin Exp Dermatol*, Vol. 25, pp. 655–656.

Malpighi, M., 1966, "Manoscritti vol XII foglio 81; in Anzalone M (ed): Marcello Malpighi e i suoi scritti sugli organi del respiro", *Bologna, Tamari*, Vol. 12, pp. 259.

Mariotta, S., L. Guidi, P. Mattia, L. Torelli, G. Pallone, G. Pedicelli and A. Bisetti, 1997a, "Pulmonary Alveolar Microlithiasis : Report of two cases", *Respiration*, Vol. 64, pp. 165-169.

Mariotta, S., L. Guidi, M. Papale, A. Ricci and A. Bisetti, 1997b, "Pulmonary Alveolar Microlithiasis : A review of Italian Reports", *European Journal of Epidemiology*, Vol. 13, pp. 587-590.

Miyoshi, K., J. M. Shillingford, G. H. Smith, S. L. Grimm, K. U. Wagner, T. Oka, J. M, Rosen, G. W. Robinson and L. Henninghausen, 2001,"Signal transducer and activator of transcription (Stat) 5 controls the proliferation and differentiation of mammary alveolar epithelium", *Journal of Cell Biology*, Vol. 155, pp. 531-542.

Mullins, T. L., G. R. Sant, A. A. Ucci and F. J. Doherty, 1986, "Testicular microlithiasis occuring in postorchiopexy testis", *Urology*, Vol. 27, pp. 144–146.

Ninis, V. N., 2003, "Genetic Studies on two brain cancers and two pulmonary alveolar diseases", *Ph. D. Thesis*, Boğaziçi University.

Nistal, M., R. Paniagua and J. A. Diez-Pardo, 1979, "Testicular microlithiasis in 2 children with bilateral cryptorchidism", *Journal of Urology*, Vol. 121, pp. 535–537.

Nouh, M. S., 1989, "Is the desert lung syndrome (nonoccupational dust pneumoconiosis) a variant of pulmonary alveolar microlithiasis", *Respiration*, Vol. 55, pp. 122-126.

Nyholt, D. R., 2000, "All LODs are not Created Equal", *American Journal of Human Genetics*, Vol. 67, pp. 282-288.

Para, B. L., D. D. Venable, L. L. Gonzalez and J. A. Eastham, 1996, "Testicular microlithiasis as a predictor of intratubular germ cell neoplasia", *Urology*, Vol. 48 pp. 797–799.

Passariello, R., 1968, “La microlitiasi alveolare del polmone: revisione della letteratura e presentazione di 6 nuovo casi”, *Riv Radiol*, Vol. 8, pp. 3-75.

Perosa, L., M. Ramunni, 1959, “La Microlithiasi endoalveolare del Polmone”, *Recenti Progr Med*, Vol. 26, pp. 354-429.

Pracyk, J. B., S. G. Simonson, S. L. Young, A. J. Ghio, V. L. Roggli,C. A. Piantadosi, 1996, “Composition of lung lavage in pulmonary alveolar microlithiasis”, *Respiration*, Vol. 63 (4), pp. 254-260.

Prakash, U. B. S., S. S. Barham, E. C. Rosenow III, M. L. Brown and W. Payne Spencer, 1983, “Pulmonary Alveolar Microlithiasis : A Review including ultrastructural and pulmonary function studies”, *Mayo Clin Proc*, Vol. 58, pp. 290-300.

Priebe, C. J. and R. Garret, 1970, “Testicular calcification in a 4-year-old boy”, *Pediatrics*, Vol. 46, pp. 785–788.

Puhr, L., 1933, “Mikrolithiasis alveolaris pulmonum”, *Virchow Arch Path Anat*, Vol. 290, pp. 156-160.

Senyigit, A., A. Yaramis, F. Gurkan, G. Kirbas, H. Buyukbayram, H. Nazaroglu, M. N. Alp and F. Topcu, 2001, “Pulmonary Alveolar Microlithiasis : A rare familial inheritance with report of six cases in a family”, *Respiration*, Vol. 68, pp. 204-209.

Stamatis, G., H. R. Zerkowski, N. Doetsch, D. Greschuchna, N. Konietzko and J. C. Reidemeister, 1993, “Sequential bilateral lung transplantation for pulmonary alveolar microlithiasis”, *Ann Thorac Surg*, Vol. 56, pp. 972-975.

Traebert, M., Hattenhauer O., Murer H., Kaissling B., Biber J., 1999, “Expression of type II Na-Pi cotransporter in alveolar type II cells”, *American Journal of Physiology*, Vol. 21, pp. 868–873.

Ucan, E. S., A. I. Keyf, R. Aydilek, Z. Yalcin, S. Sebit, M. Kudu and U. Ok, 1993, "Pulmonary Alveolar Microlithiasis : Review of Turkish Reports", *Thorax*, Vol. 48, pp. 171-173.

Vegni-Talluri, M., E. Bigliardi, M. G. Vanni and G. Tota, 1980, "Testicular microliths: their origin and structure", *Journal of Urology*, Vol. 124, pp. 105–107.

Weissenbach, J., G. Gyapay, C. Dib, A. Vignal, J. Morissette, P. Millasseau, G. Vaysseix and M. Lathrop, 1992, "A Second Generation Linkage Map of the Human Genome", *Nature*, Vol. 359, pp. 794-801.

Wineselberg, G. G., M. Boller and M. Sachs, 1984, "CT evaluation in pulmonary alveolar microlithiasis", *Journal of Computer Assisted Tomography*, Vol. 22, pp. 245-248.

Xu, H., J. F. Collins, L. Bai, P. R. Kiela, and F. K. Ghishan, 2001, "Regulation of the human sodium-phosphate cotransporter NaP_i-IIb gene promoter by epidermal growth factor", *American Journal of Physiology*, Vol. 280, pp. C628–C636.

Yeo, G., S. Hoon,B. Venkatesh, C. B. Burge, 2004, "Variation in sequence and organization of splicing regulatory elements in vertebrate genes", *Proc Natl Acad Sci*, Vol. 101, pp. 15700-15705.